



SCHOOL of  
GRADUATE STUDIES  
EAST TENNESSEE STATE UNIVERSITY

East Tennessee State University  
Digital Commons @ East  
Tennessee State University

Electronic Theses and Dissertations

Student Works

8-2014

# Synthesis and Characterization of [VO(O<sub>2</sub>)H<sub>2</sub>EDTA] and Investigation of the Reaction Between [VOHEDTA]<sup>-1</sup> and Hydrogen Peroxide as a Model Catalyst for Haloperoxidases

Tinga C. O. Fon Mr.

*East Tennessee State University*

Follow this and additional works at: <https://dc.etsu.edu/etd>

 Part of the [Chemistry Commons](#)

## Recommended Citation

Fon, Tinga C. O. Mr., "Synthesis and Characterization of [VO(O<sub>2</sub>)H<sub>2</sub>EDTA] and Investigation of the Reaction Between [VOHEDTA]<sup>-1</sup> and Hydrogen Peroxide as a Model Catalyst for Haloperoxidases" (2014). *Electronic Theses and Dissertations*. Paper 2424. <https://dc.etsu.edu/etd/2424>

This Thesis - Open Access is brought to you for free and open access by the Student Works at Digital Commons @ East Tennessee State University. It has been accepted for inclusion in Electronic Theses and Dissertations by an authorized administrator of Digital Commons @ East Tennessee State University. For more information, please contact [digilib@etsu.edu](mailto:digilib@etsu.edu).

Synthesis and Characterization of [VO(O<sub>2</sub>)H<sub>2</sub>EDTA] and Investigation of the Reaction Between  
[VOHEDTA]<sup>-1</sup> and Hydrogen Peroxide as a Model Catalyst for Haloperoxidases

---

A thesis  
presented to  
the faculty of the Department of Chemistry  
East Tennessee State University

In partial fulfilment  
of the requirement for the degree  
Master of Science in Chemistry

---

by  
Tinga Clifford Oyombe Fon  
August 2014

---

Dr. Jeffrey Wardeska, Chair

Dr. Scott Kirkby

Dr. Cassandra T. Eagle

Keywords: Vanadiumhaloperoxidase, Oxoperoxocomplexes, Oxibromination

## ABSTRACT

Synthesis and Characterization of  $[\text{VO}(\text{O}_2)\text{H}_2\text{EDTA}]$  and Investigation of the Reaction Between  $[\text{VOHEDTA}]^{-1}$  and Hydrogen Peroxide as a Model Catalyst for Haloperoxidases

by

Tinga Clifford Oyombe Fon

Vanadium haloperoxidases (VHPOs) are enzymes that catalyse the oxidation of halide ions to hypohalous acids by hydrogen peroxide. There are many unanswered questions on the mechanism by which the oxidation reaction occurs. In this work, is reported the synthesis of  $[\text{VO}(\text{O}_2)\text{H}_2\text{EDTA}]$ , studies of the effect of acid concentration on the decomposition of  $[\text{VO}(\text{O}_2)\text{HEDTA}]^{-2}$ , and mechanistic studies of the rate law. The decomposition reaction was found to be first order with respect to acid concentration and also  $[\text{VO}(\text{O}_2)\text{HEDTA}]^{-2}$  concentration. The reaction of  $[\text{VOHEDTA}]^{-1}$  and hydrogen peroxide progressed *via* a free radical path way. In addition, the vanadium(V) complex  $[\text{VO}(\text{O}_2)\text{H}_2\text{EDTA}]$  was synthesized and characterised by FT-IR, UV-VIS and GC-MS. The catalytic properties of  $[\text{VO}(\text{O}_2)\text{H}_2\text{EDTA}]$  were investigated for an oxibromination reaction. It was found that the catalysed, and the control reaction showed no major differences except for the fact that the reaction with the catalyst gave a dibrominated product without a carbonyl group.

## TABLE OF CONTENTS

|   | Page |
|---|------|
| ABSTRACT .....  | 2    |
| LIST OF TABLES .....  | 6    |
| LIST OF FIGURES.....  | 7    |
| LIST OF ABBREVIATIONS.....                                      | 9    |
| Chapter   |      |
| 1. INTRODUCTION .....   | 10   |
| A General Review on Vanadium and Vanadium Peroxocomplexes ..... | 10   |
| Methods of Preparation of Vanadium Peroxycompounds.....         | 14   |
| Structure of Vanadium Peroxocomplexes .....                     | 19   |
| Monoperoxocomplexes .....                                       | 19   |
| Diperoxo Complexes.....   | 20   |
| TriperoxoComplexes.....   | 21   |
| Characteristic Spectrum of Vanadium Peroxocomplexes.....        | 22   |
| Electron Absorption and UV-Visible Spectroscopy.....            | 22   |
| FT-IR Spectroscopy .....  | 24   |

|   |    |
|---|----|
| Vanadium Hydrogen Peroxide Reaction .....   | 25 |
| Vanadium Haloperoxidases .....  | 25 |
| Goals for this Research .....   | 28 |
| 2. METHODOLOGY.....   | 29 |
| Materials and Reagents.....   | 30 |
| Reagent .....   | 30 |
| Materials .....   | 30 |
| Preparation of Solutions and Complexes.....   | 32 |
| Preparation of $[\text{VOHEDTA}]^{-1}$ Solution.....  | 32 |
| Reaction of $[\text{VOHEDTA}]^{-1}$ with $\text{H}_2\text{O}_2$ .....   | 33 |
| Initial Rate Study of the Effect of $[\text{H}^+]$ on the Decomposition<br>of $[\text{VO}(\text{O}_2)\text{HEDTA}]^{-2}$ in Solution..... | 33 |
| Synthesis of $[\text{VO}(\text{O}_2)\text{H}_2\text{EDTA}]$ .....   | 33 |
| Test for the Catalytic Properties of $[\text{VO}(\text{O}_2)\text{H}_2\text{EDTA}]$ .....   | 34 |
| Electronic Absorption, UV-Visible, Studies.....   | 35 |
| Gas Chromatography Mass Spectrometry Studies.....   | 35 |
| Fourier Transform Infrared Spectroscopy Studies.....  | 36 |

|   |    |
|---|----|
| 3. RESULTS .....  | 37 |
| Preparation of Solutions and Complexes .....  | 37 |
| Spectrum For the Reaction Between $[\text{VO}(\text{HEDTA})]^{-1}$ and $\text{H}_2\text{O}_2$ .....   | 39 |
| Initial Rate Study of the Effect of $[\text{H}^+]$ on $[\text{VO}(\text{O}_2)\text{HEDTA}]^{-2}$ in Solution .....                          | 42 |
| A Fixed Concentration of $[\text{VO}(\text{O}_2)\text{HEDTA}]^{-2}$ while Concentration<br>of Acid is Varied .....                          | 42 |
| A fixed Concentration of Acid While the Concentration of<br>$[\text{VO}(\text{O}_2)\text{HEDTA}]^{-2}$ is Varied .....                      | 45 |
| Calculating The Rate Constant While Changing the Concentrations of<br>Acid and $[\text{VO}(\text{O}_2)\text{HEDTA}]^{-2}$ in Solution ..... | 47 |
| Studies on the Catalytic Properties of $[\text{VO}(\text{O}_2)\text{H}_2\text{EDTA}]$ .....   | 50 |
| 4. DISCUSSION .....   | 61 |
| Future Work .....   | 65 |
| REFERENCES .....  | 66 |
| APPENDIX: Standardization of $\text{KMnO}_4$ and $\text{VO}^{2+}$ Solutions .....   | 69 |
| VITA .....  | 71 |

## LIST OF TABLES

| Table  | Page |
|--|------|
| 1. Electronic Absorption Spectra Data for Structurally Characterized Hetero Ligand Monoperoxidovanadium(V) Complexes ..... | 23   |
| 2. Volume of Acid, Concentration of $[H^+]$ and Initial Rates .....  | 43   |
| 3. The Initial Rates, pH, and Concentrations for the Various Volumes of Solution ...                                       | 46   |
| 4. The Initial Rates and Concentration for the Various Volume of Solution.....   | 48   |
| 5. Results for Elemental Analysis for $[VO(O_2)H_2EDTA]$ .....   | 53   |
| 6. Summary of the Results from GC-MS Analysis of Reaction Without a Catalyst.....  | 60   |
| 7. Summary of the Results from GC-MS Analysis of Reaction with Catalyst.....   | 60   |

## LIST OF FIGURES

| Figure   | Page |
|--|------|
| 1. Four “free” positions ( $e_1$ , $e_2$ , $e_3$ and a) for coordination of the donor atoms to the $\text{VO}(\text{O}_2)^+$ Moiety .....                        | 20   |
| 2. Structure of $[\text{VO}(\text{O}_2)_2]^{-1}$ .....   | 21   |
| 3. Structure of $[\text{V}(\text{O}_2)_3]^{-1}$ .....  | 21   |
| 4. UV-visible spectrum of $(\text{H}_3\text{O})_2[\text{V}_2(\text{O})_2(\text{O}_2)_4(\text{C}_2\text{H}_5\text{NO}_2)]$ in water.....                          | 24   |
| 5. IR spectrum of $[\text{Ni}(\text{NH}_3)_6][\text{VO}(\text{O}_2)(\text{NH}_3)]_2$ .....   | 24   |
| 6. Structure of the active side of vanadium containing haloperoxidase .....  | 26   |
| 7. The UV-Visible spectrum of $\text{VO}(\text{ClO}_4)_2$ solution .....   | 37   |
| 8. The UV-Visible spectrum of $[\text{VO}(\text{HEDTA})]^{-1}$ solution.....   | 38   |
| 9. The UV-Visible spectrum for the reaction between $[\text{VO}(\text{HEDTA})]^{-1}$ and $\text{H}_2\text{O}_2$ showing the progress of the reaction path.....   | 39   |
| 10. A plot of the absorbance at 425 nm against time for the reaction between $[\text{VO}(\text{HEDTA})]^{-1}$ and $\text{H}_2\text{O}_2$ .....                   | 40   |
| 11. The UV-Visible spectrum of $[\text{VO}(\text{O}_2)\text{HEDTA}]^{-2}$ solution.....  | 41   |
| 12. A plot of absorbance at 425 nm against time in seconds for all four volumes of solution.....   | 43   |
| 13. Plot of initial rates against concentration of $[\text{H}^+]$ for the plot of concentration of $[\text{VO}(\text{O}_2)\text{HEDTA}]^{-2}$ against time ..... | 44   |
| 14. A plot of initial rate against concentration of $[\text{VO}(\text{O}_2)\text{HEDTA}]^{-2}$ .....   | 45   |



|   |    |
|---|----|
| 15. Plot of concentration of $[\text{VO}(\text{O}_2)\text{HEDTA}]^{-2}$ against time .....  | 46 |
| 16. A plot of initial rate against concentration of $[\text{VO}(\text{O}_2)\text{HEDTA}]^{1-2}$ .....                               | 48 |
| 17. UV-Visible spectrum of $[\text{VO}(\text{O}_2)\text{HEDTA}]^{-2}$ solution five days after<br>reacting with acid.....           | 49 |
| 18. Structure of $\text{H}_3\text{EDTA}$ .....  | 50 |
| 19. FT-IR spectrum of $\text{H}_3\text{EDTA}$ .....   | 51 |
| 20. FT-IR spectrum of $[\text{VO}(\text{O}_2)\text{H}_2\text{EDTA}]$ .....  | 51 |
| 21. The UV-Visible spectrum of $[\text{VO}(\text{O}_2)\text{HEDTA}]^{-2}$ in DMSO.....  | 52 |
| 22. The GC-MS of the oxibromination reaction of salicylaldehyde without the<br>catalyst .....                                       | 53 |
| 23. The GCMS of the oxibromination reaction of salicylaldehyde with a catalyst.....   | 54 |
| 24. MS spectrum for peak at 6.674 min.....  | 55 |
| 25. MS spectrum for peak at 9.116 min for reaction without catalyst.....  | 55 |
| 26. The MS Spectrum for peak at 9.743 min for reaction without catalyst.....  | 56 |
| 27. The MS spectrum for peak at 9.118 min for reaction with catalyst .....  | 56 |
| 28. The spectrum for the peak at 11.40 min for the reaction without catalyst .....  | 57 |
| 29. The MS spectrum for the peak at 11.416 min for the reaction without catalyst....  | 57 |
| 30. Fragmentation patterns for peaks with m/z of 280 .....  | 57 |
| 31. Fragmentation patterns for peaks with m/z 280 .....   | 58 |
| 32. The GCMS of the oxibromination reaction of salicylaldehyde with a catalyst<br>for the peak at 9.730 min with an m/z of 252..... | 59 |
| 33. The structure of $[\text{VO}(\text{O}_2)\text{H}_2\text{EDTA}]$ .....   | 64 |

## LIST OF ABBREVIATIONS

|       |  |
|-------|--|
| THF   | Tetrahydrofuran  |
| BHT   | Butylated hydroxytoluene                                 |
| BFMH  | Benzoic acid(phenylmethylene)hydrazide                   |
| BAMH  | Benzoic acid[1-(anisol-3-yl)methylene]hydrazide          |
| BTMH  | Benzoic acid[(thiophene-2-yl)methylene]hydrazide         |
| BPMH  | Benzoic acid(phenylmethylene)hydrazide                   |
| PAV   | Poly(acrylate)   |
| PMAV  | Polymethacrylate   |
| PA    | poly(acrylate)   |
| PMA   | Polymethacrylate   |
| LMCT  | Ligand to metal charge transfer                          |
| FT-IR | Fourier transform infrared                               |
| VHPOs | Vanadium haloperoxidases                                 |
| DMSO  | Dimethyl sulfoxide                                       |
| GCMS  | Gas chromatography mass spectrometry                     |
| HEDTA | N-(2-Hydroxyethyl)ethylenediamine-N,N',N'-triacetic acid |

## CHAPTER 1

### INTRODUCTION

#### A General Review on Vanadium and Vanadium Peroxocomplexes

In this literature review, the main focus is on the peroxocomplexes of vanadium. Before diving into the peroxocomplexes of vanadium, it is of importance to first look at some aspects of vanadium as a metal. In 1801, Del Rio discovered vanadium as element 23, which coexisted in lead ore. He gave it the name panchromium and later changed it to erythronium.<sup>1</sup> Based on wrong results from Collett De Sotils, his claims were withdrawn. Later, in 1830, the Swedish chemist Sefström rediscovered the element. The element was named vanadin and later changed to the Latin name vanadium. The name vanadium came from the Nordic goddess of beauty Vanadis because of its beautifully coloured compounds.<sup>1,2,3</sup> In 1867, Roscoe became the first person to produce the metal in an acceptably clean form by reducing the metal chloride with hydrogen.<sup>4,5</sup> Vanadium is in period 4 and group 5 of the periodic table, is soft and grey in colour, and has a ground state electron configuration of  $[\text{Ar}] 4s^2 3d^3$ . It has two isotopes,  $^{51}\text{V}$  (99.76%) and  $^{50}\text{V}$  (0.24%); its most common ions have oxidation states +III, +IV, and +V. Vanadium-50 is radioactive with a half-life of six quadrillion years.<sup>5</sup> It is the 19<sup>th</sup> most abundant element in the earth's crust with an estimated concentration of 0.014%. This also makes it the 5<sup>th</sup> most common transition metal.<sup>5</sup> Vanadium is found in crude oil in Venezuela and Canada and also in a few other deposits around the world. Vanadium is the second most abundant transition metal in seawater with a concentration of about 20.53 nM.<sup>1,2,3,4,5</sup> There are about 65 minerals containing vanadium but very few concentrated deposits. Vanadium is found in small amounts that are associated with deposits of lead, lead-zinc, and lead-copper. Vanadium containing minerals that

are considered to be the most important are: vanadinite ( $3\text{Pb}_3(\text{VO}_4)_2 \cdot \text{PbCl}_2$ ), patronite, the polysulphide,  $\text{VS}_4$ , carnotite,  $\text{K}(\text{UO}_2)(\text{VO}_4)1 \cdot 5\text{H}_2\text{O}$ , mottramite,  $(\text{Pb,Ca,Cu})_3(\text{VO}_4)_2$ , roscoelite ( $2\text{K}_2\text{O} \cdot 2\text{Al}_2\text{O}_3 \cdot (\text{Mg,Fe})\text{O} \cdot 3\text{V}_2\text{O}_5 \cdot 10\text{SiO}_2 \cdot 4\text{H}_2\text{O}$ ), descloizite,  $(\text{Pb,Zn})_3(\text{VO}_4)_2$ , and tyuyamunite,  $(\text{Ca}(\text{UO}_2 \cdot \text{VO}_4)_2 \cdot 4\text{H}_2\text{O})$ . The pure metal is produced by reduction of chlorides, reduction of oxide, and thermal dissociation of the diiodide.<sup>4</sup> A high purity metal may be obtained by electrorefining calcium-reduced vanadium in chloride or bromide electrolytes. Vanadium shows good characteristics of corrosion resistance to salt water, to air at ordinary temperatures, to hydrochloric and sulphuric acids, and to alkalis.<sup>4</sup> Vanadium is corroded by concentrated hydrofluoric, sulphuric, and nitric acids. It will combine with most nonmetals at high temperatures. About 90% of all vanadium produced is used in the production of steel.<sup>5</sup> Vanadium makes the steel stronger, tougher, and more rust resistant.<sup>5</sup> Alloys of vanadium are used in the manufacture of space vehicles, aircraft, in cutting and grinding tools, and in building and heavy construction.<sup>5</sup> Vanadium in compounds such as vanadium pentoxide, vanadium peroxide, etc., is used as a catalyst in some industrial reactions.<sup>5</sup> Vanadium compounds are also used as colouring additives in glass and ceramics and as dyes in textiles.<sup>5</sup> There is an increasing use of vanadium in the manufacture of smaller and lighter batteries for electrically powered automobile use and space shuttles.<sup>4</sup> Vanadium pentoxide batteries produce more electrical energy per pound than lead storage batteries.<sup>4,5</sup>

The vanadium(III) oxidation state has stability only over a limited pH and potential range in aqueous solutions. In a hydrolytic reaction, monomeric  $[\text{V}(\text{OH})_n(\text{H}_2\text{O})_{6-n}]^{(3-n)+}$  species are formed where  $n = 0-3$ .<sup>1</sup> Higher nuclearity dimeric and trimeric species are also formed with all

the species being cationic. In the presence of strong reducing ligands such as picolinate, alanine, serine, lactate etc. In aqueous solution, stable vanadium(III) complexes are formed.<sup>1</sup>

Vanadium(IV) yields cationic species when hydrolysed. The vanadyl cation is denoted as  $\text{VO}^{2+}$ . In hydrated form it is stable as  $[\text{VO}(\text{H}_2\text{O})_5]^{2+}$ . The vanadium(IV) compounds are referred to as vanadyl species. Vanadyl cations are stable in very acidic solutions and are stored in the presence of air without being oxidised. As the pH increases, different oligomeric and polymeric species begin to form, such as  $(\text{VO})_2(\text{OH})_2^{2+}$  that forms between pH 4 and 11. Vanadium(IV) oxide ( $\text{V}_2\text{O}_4$ ) has a very low solubility and will precipitate. Precipitation and polymerisation are prevented by complex formation as vanadium has a high affinity for most N-, O- and S-donor ligands.  $\text{VO}^{2+}$  also acts as a simple divalent ion and competes with  $\text{Ca}^{2+}$ ,  $\text{Mn}^{2+}$ ,  $\text{Zn}^{2+}$  in certain proteins for binding sites.<sup>1</sup>

Vanadium(V) forms anionic species with the exception of pervanadyl ion ( $\text{VO}_2^+$ ) formed in very acidic solution ( $\text{pH} < 3$ ) that has a pale yellow colour. Metavanadate ion,  $(\text{VO}_3)_n^{n-}$ , exists only in the solid state and dissolves in water to form a mixture of mono-, and oligovanadates. The type of vanadate formed is dependent on the pH, the ionic strength of the medium, and total concentration of vanadium. When the pH of the solution is increased to between 3 and 6, the decavanadates dominate, which have an orange colour. The decavanadates have a general formula of  $\text{H}_n\text{V}_{10}\text{O}_{28}^{(6-n)-}$ , where  $n = 0 - 3$ , and are abbreviated  $\text{V}_{10}$ . Vanadium atoms have an octahedral coordination and are classified in terms of their position in the structure as corner, (4 atoms), capping, (4) or central (2). At the metavanadate range, which is the neutral pH range, mono-, di-, and cyclic, colourless oligovanadates are formed. The species  $\text{H}_2\text{VO}_4^-$  (denoted as  $\text{V}_1$ ),  $\text{H}_2\text{V}_2\text{O}_7^{2-}$  ( $\text{V}_2$ ),  $\text{V}_4\text{O}_{12}^{4-}$  ( $\text{V}_4$ ), and  $\text{V}_5\text{O}_{15}^{5-}$ , ( $\text{V}_5$ ), have a charge of -1 each per vanadium with

the vanadium being tetrahedrally coordinated to oxygen. When the pH is raised to  $\text{pH} > 8$ ,  $\text{HV}_4\text{O}_{13}^{5-}$  and  $\text{V}_4\text{O}_{13}^{6-}$  are formed. These are linear trimeric species. These conditions also favour the formation of  $\text{HV}_2\text{O}_7^{3-}$ , a dimer which is singly deprotonated. In more alkaline solutions, the most common species are  $\text{HVO}_4^{2-}$ , which is a monoprotonated monomer and  $\text{V}_2\text{O}_7^{4-}$ , which is its dimer. The vanadate ion  $\text{VO}_4^{3-}$  is the only species at  $\text{pH} > 12$ .<sup>1</sup>

Theoretical studies have shown that vanadium meets several criteria to be considered an essential nutrient.<sup>3</sup> These criteria include low molecular weight, excellent catalytic activity, homeostatic regulation by controlled accumulation, and low toxicity on oral intake.<sup>3</sup> Studies have shown that vanadium deficiency leads to pathology. Some effects of vanadium deficiency include miscarriage and perinatal mortality, bone abnormalities, and changes in thyroid metabolism.<sup>3</sup>

Research on vanadium complexes has intensified since 1979 when Tolman and colleagues brought to the limelight the insulin mimetic action of vanadium.<sup>3</sup> Their discoveries, and later supportive discoveries, have shown that vanadium can be considered as an insulin mimicking compound that may control glucose metabolism either by an insulin-dependent and/or independent biochemical pathway.<sup>3</sup> Compounds of peroxovanadium(V) complexes have enormous potentials as medicinal and inorganic functionalised materials. These compounds have been investigated and have shown evidence of insulin mimetic activities and antitumor function. They have been studied for use as functional models for the vanadium haloperoxidase enzymes.<sup>6</sup> These enzymes catalyse the oxidation of halides by hydrogen peroxide and are thought to be involved in the biosynthesis of a large number of marine natural products, many of them with potential antifungal, antibacterial, antiviral, and antineoplastic properties.<sup>3,6,7</sup>

Our interest in vanadium is due to its peroxycomplexes and their importance in biomedical and catalytic applications. A number of oxidation reactions may be efficiently performed by peroxovanadium(V) complexes. These complexes have the potential to hydroxylate benzene and other aromatics and aliphatic hydrocarbons, epoxides, hydroxylate alkenes, and allylic alcohols and oxidize sulphides and primary and secondary alcohols.<sup>3, 6-8</sup> These processes and reactions, which are either stoichiometric or catalytic, and where the oxidant can either be alkylhydroperoxide or hydrogen peroxide are usually carried out in mild conditions, give good product yields, and also show high selectivity.<sup>9</sup> Vanadium peroxide complexes have been studied in many forms ranging from the oxo-peroxo, mono-peroxo, diperoxo, triperoxo, and species to complexes with two or more metal centres.

#### Methods of Preparation of Vanadium Peroxycompounds

Tatiersky and colleagues composed a review on monoperoxovanadium(V) complexes and established the following conditions for synthesis of vanadium(V) complexes<sup>10</sup>, vanadium compound-H<sub>2</sub>O<sub>2</sub>-ligand/solvent. They also established that V<sub>2</sub>O<sub>5</sub>, NH<sub>4</sub>VO<sub>3</sub> or KVO<sub>3</sub>, VOSO<sub>4</sub> or VCl<sub>3</sub> are the most commonly used starting compounds for vanadium complexes. Dissolving vanadium pentoxide usually requires cooling in an ice bath either in a dilute solution of hydrogen peroxide or an aqueous solution of a base. Alternatively, dissolving vanadium pentoxide in a base may require gentle heating. Solid ligands may be added to the reaction system or a solution of the ligand in water or any appropriate organic solvent such as acetonitrile, ethanol, or methanol. Acids such as perchloric acid or hydrochloric acid or bases such as alkali hydroxides or ammonia may be used to adjust the pH when necessary. Very acidic solutions with pH ranging between 0.3 and 1.7 give cationic monoperoxido complexes of the form [VO(O<sub>2</sub>)(L)]<sup>n+</sup>.

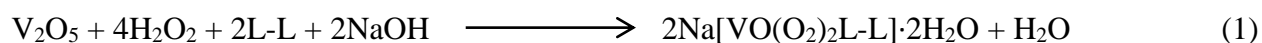
Less acidic solutions of pH range 1.2 to 2.2 give neutral complexes of the form  $[\text{VO}(\text{O}_2)(\text{L})]$ . A pH of 1.8 yields anionic complexes of form  $[\text{VO}(\text{O}_2)(\text{L})]^{n-}$ . The complexes are usually crystallized by adding an organic cosolvent such as ethanol or methanol in small amounts in order not to form a stable precipitate. Crystalline products are formed at a temperature range between -70 °C to 25 °C, which may be stable for hours to weeks or even months.<sup>10</sup>

In this review, a selection of synthetic routes for vanadium(V) peroxocomplexes that include mono-, di-, triperoxides, and some complexes with more than one metal centre is presented. Vanadium peroxocompounds are generally prepared by reacting vanadium(IV) or vanadium(V) compounds with hydrogen peroxide or alkyl peroxides.<sup>10</sup>

Waidmann and colleagues, in an attempt to synthesise the peroxo compound,  $[\text{V}^{\text{V}}(\text{O}_2)\cdot(4,4\text{-Bu}_2\text{-bpy})_2]\text{BF}_4$ ,  $\text{V}^{\text{V}}(\text{O}_2)$ , ended up with an oxo-peroxo-vanadium(V) species;  $[\text{V}^{\text{V}}\text{O}(\text{O}_2)(\text{Bu}_2\text{bpy})_2]\text{BF}_4$ , abbreviated  $[\text{V}^{\text{V}}\text{O}(\text{O}_2)]$ .<sup>7</sup> In their synthesis, while exposing vanadium(IV) to air, the hydroxo complex  $[\text{V}^{\text{IV}}\text{O}(\text{OH})(\text{Bu}_2\text{bpy})_2]\text{BF}_4$ ,  $[\text{V}^{\text{VI}}\text{O}(\text{OH})]$  was stirred in THF. After three days at ambient temperatures, the partially soluble yellow suspension of  $\text{V}^{\text{VI}}(\text{OH})$  in THF was transformed into a red suspension. On addition of pentane, a pale red solid of oxo-peroxo-vanadium(V)  $[\text{V}^{\text{V}}\text{O}(\text{O}_2)(\text{Bu}_2\text{bpy})_2]\text{BF}_4$ ,  $[\text{V}^{\text{V}}\text{O}(\text{O}_2)]$  was obtained in a 97% yield. The use of either 1 atm. of air or 1 atm. of dry oxygen gave a high yield. The reaction has a good profile in dry THF distilled from Na/Ph<sub>2</sub>CO, or in wet unpurified THF from a bottle containing 250 ppm of the stabilizer BHT (butylated hydroxytoluene, 2, 6-Bu<sub>2</sub>-4-Me-C<sub>6</sub>H<sub>2</sub>OH). By their research, it was observed that  $\text{V}^{\text{IV}}\text{O}(\text{OH})$  converts to  $\text{V}^{\text{V}}\text{O}(\text{O}_2)$  only in the presence of oxygen and ethereal solvent.<sup>7</sup>



Mahajan and colleagues synthesized peroxo complexes of vanadium(V) containing aroylhydrazone ligands of benzoic acid [1-(Furan-2-yl)methylene]hydrazide (BFMH),<sup>8</sup> benzoic acid[(thiophene-2-yl)methylene]hydrazide (BTMH), benzoic acid(phenylmethylene)hydrazide(BPMH), benzoic acid[1-(anisol-3-yl)methylene]hydrazide (BAMH), benzoic acid[1-(thiophene-2-yl)ethylidene]hydrazide (BTEH), benzoic acid[P-chlorobenzylmethylene]hydrazide (BCMh) in separate complexes with each as a ligand.<sup>8</sup> In their syntheses, solid V<sub>2</sub>O<sub>5</sub> (0.25 g, 1.37 mmol) was stirred with methanolic solution of aroylhydrazones (2.74 mmol); BFMH (0.587 g), BTEH (0.669 g), BTMH (0.631 g), BPMH (0.614 g), BAMH (0.697 g) and BCMH (0.709 g). Hydrogen peroxide (12 mL of 30%, 105.84 mmol) was added to each of these solutions gradually with constant stirring. The temperature was kept below 4 °C in an ice bath. The mixture was stirred until all the solids were dissolved. The pH at this stage was measured to be ca. 6, it was then raised to 10 by drop-wise addition of dilute sodium hydroxide solution (0.1 M) while stirring. Precooled ethanol (about 50 mL) was added to the mixture with constant vigorous stirring and a yellow paste was separated. The reactions were allowed to stand in an ice bath for 15 minutes, which produced light colored precipitates. These were then filtered, repeatedly, washed with acetone, and then dried at room temperature in *vacuo* over calcium chloride.<sup>8</sup>



Where, L-L= BFMH, BTEH, BTMH, BPMH, BAMH and BCMH

Chakravorti and colleagues electro-synthesised peroxyvanadium(V) complexes by the method of a sacrificial anode. The electrochemical cell was made up of a vanadium pellet anode that was connected to a platinum foil of dimensions 1 x 1 x 0.05 cm as the cathode. By

electrochemical synthesis,  $\text{H}[\text{VO}(\text{O}_2)_2\text{L}]$  and  $\text{LH}_2[\text{VO}(\text{O}_2)_2\text{L}]_2 \cdot 6\text{H}_2\text{O}$  in which L is 2,2-bipyridine or 1,10-phenanthroline were produced. An electrolytic cell was run for 3 hours at a temperature between 0 and 5 °C in which 10 cm<sup>3</sup> of 30% hydrogen peroxide with the vanadium pellets and the platinum foil each connected to platinum wire in the presence of an electrolyte, tetrabutylammonium perchlorate (0.05 g), at a current voltage of 4 V and 0.1 amps. The electrolysis gave a deep red solution which was filtered to remove any metal particles.

Calculations for the amount of metal lost preceded the addition of an ethanolic solution of 2,2-bipyridine or 1,10-phenanthroline to the filtrate at a temperature range of 0 to 5 °C. When the ratio of V:L was 1:3,  $\text{H}[\text{VO}(\text{O}_2)_2\text{L}]$  was precipitated, by maintaining the ratio of vanadium to that of L at 1:1.  $\text{LH}_2[\text{VO}(\text{O}_2)_2\text{L}]_2 \cdot 6\text{H}_2\text{O}$  was precipitated,  $\text{K}_3[\text{VO}(\text{O}_2)_2(\text{C}_2\text{O}_4)] \cdot \text{H}_2\text{O}$  and  $\text{K}[\text{VO}(\text{O}_2)_2\text{L}]_2 \cdot 6\text{H}_2\text{O}$  were synthesised by repeating the electrolysis process as described above, and then adding  $\text{K}_2\text{C}_2\text{O}_4$  in a ratio of 1:1 to the concentration of vanadium. The pH of the solution was raised to 7 by adding KOH solution and a minimum volume of ethanol added to precipitate  $\text{K}_3[\text{VO}(\text{O}_2)_2(\text{C}_2\text{O}_4)] \cdot \text{H}_2\text{O}$ . The synthesis of  $\text{K}[\text{VO}(\text{O}_2)_2(\text{H}_2\text{O})]$  was accomplished by raising the pH of the solution left after electrolysis to 7 and then adding ethanol to it. When the electrolysis was carried out in 0.6 g (0.010 mol) KOH and 5 cm<sup>3</sup> (0.049 mmol) of 30%  $\text{H}_2\text{O}_2$  at 0 °C, a blue solution was the product.  $\text{K}[\text{V}(\text{O}_2)_3] \cdot 3\text{H}_2\text{O}$  was precipitated out of the blue solution by the addition of ethanol. Filtration was the separation method for all the complexes; they were washed with ethanol and dried in vacuo over concentrated sulphuric acid.<sup>12</sup> The Chakravorti group also applied a chemical method in their synthesis of peroxo vanadium complexes.<sup>12</sup> To 30% hydrogen peroxide, was added finely powdered vanadium, and the mixture was allowed to stand for 4 to 5 hours at a temperature range between 0 to 5 °C while stirring occasionally. This resulted in a red solution from which the metal particles were filtered. The resulting diperoxo

complexes were obtained from the filtrate by the same procedure as already described above. The complex  $K[V(O_2)_3] \cdot 3H_2O$  was chemically synthesised by stirring 0.25 g (0.0049 mmol) of vanadium powder, 10 cm<sup>3</sup> of 30% (0.97 mmol) hydrogen peroxide and 1.5 g (0.026 mmol) of KOH at 0 °C. The resulting solution was filtered and the complex obtained by adding ethanol to the filtrate.<sup>12</sup>

Kalita and his colleagues synthesised polymer bound peroxovanadium compounds  $Na_3[V_2O_2(O_2)_4(\text{carboxylate})]$  PA, [PA = poly(acrylate)] (PAV), and  $Na_2[VO(O_2)_2(\text{carboxylate})]$  PMA [PMA = polymethacrylate] (PMAV).<sup>12</sup> These were prepared by gradually adding 12 ml (0.12 mol) of 30% H<sub>2</sub>O<sub>2</sub> solution that contained 105.8 mM of H<sub>2</sub>O<sub>2</sub> to a mixture of 0.36 g V<sub>2</sub>O<sub>5</sub> (2.0 mmol) and with continuous stirring, 1.5 g of the various polymers dissolved in a minimum volume of water. The mixture was stirred continuously for about 30 min, until the entire solid dissolved while keeping the temperature below 4 °C in an ice bath. After all the solid had dissolved, the pH of the solution was measured to be 3, by drop wise addition of 8.0 M sodium hydroxide, the pH was raised to 6 then 50 mL of precooled acetone was added to the mixture under vigorous stirring, which gave a yellow colour pasty mass. The reaction mixture was allowed to stand for 20 min in an ice bath after which the supernatant liquid was decanted and the residue treated with acetone repeatedly while scratching until a microcrystalline solid was formed. Centrifugation was the separation method used to separate the product; it was washed with cold acetone and dried in vacuo over concentrated sulphuric acid.<sup>12</sup>

Chrappova and colleagues also synthesised  $[Zn(NH_3)_4][VO(O_2)_2(NH_3)]_2$ .<sup>13</sup> Ammonium vanadate, NH<sub>4</sub>VO<sub>3</sub>, 0.580 g (5.00 mmol) was added to 30 mL of an aqueous solution of 25% NH<sub>3</sub> followed by stirring for 30 min. ZnSO<sub>4</sub>·7H<sub>2</sub>O, 2.15 g was added to the mixture and it dissolved.

5.0 mL of 30% H<sub>2</sub>O<sub>2</sub> (50 mmol) was drop wise added to the solution obtained. A green solution was formed that was then cooled for 5 min at -30 °C and stored at -5 °C. The colour of the solution changed to yellow after about 45 min. The solution was allowed to stand for 48 hours after which 10 mL of 95% ethanol was added. After 24 hours, a yellow crystalline product was isolated, washed with ethanol, and dried at 5 °C.<sup>13</sup>

### Structure of Vanadium Peroxocomplexes

#### Monoperoxocomplexes

Tatiersky and colleagues reviewed all 72 monoperoxocomplexes that had been structurally characterized as of the year 2009.<sup>10</sup> It was established by their studies that most monoperoxocomplexes with a heptacoordinated mononuclear vanadium molecular structure have a distorted pentagonal bipyramidal structure. In these structures, the  $\eta^2$ -peroxo and the *cis* oxido ligand occupy three positions in the coordination polyhedron. This forms the central VO(O<sub>2</sub>)<sup>+</sup> moiety. The vanadium to oxido oxygen bond (V=O) has an approximate bond length of 1.6 Å and shows a partially triple bond character. The vanadium and peroxo oxygen bond also show a partially multiple character. The pentagonal plane of the molecule is defined by the peroxide oxygen atoms and donor atoms as shown in equatorial positions e<sub>1</sub>, e<sub>2</sub>, and e<sub>3</sub> in Figure 1 below. The vanadium atom is displaced towards the triply bonded oxido ligand by approximately 0.20 - 0.25 Å away from the least square pentagonal plane. The weakest bond is the bond between the vanadium atom and the donor atom *trans* to the oxido ligand, the donor atom is either oxygen or nitrogen, which is in the axial position “a” as shown in Figure 1 below. The free positions e<sub>1</sub> to e<sub>3</sub> in the pentagonal bipyramidal position are occupied by heteroligands that can be tridentate

plus a monodentate, bidentate plus two monodentate, two bidentate or tetradentate ligands that have a total donor set of  $N_xO_y$ .<sup>10</sup>

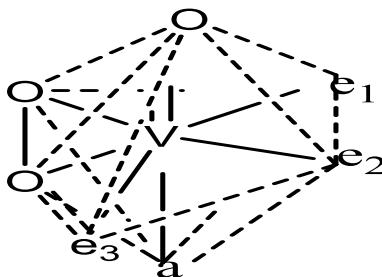


**Figure 1:** Four “free” positions ( $e_1$ ,  $e_2$ ,  $e_3$  and  $a$ ) for coordination of the donor atoms to the  $VO(O_2)^+$  moiety

The following empirical rules were established after analysing the occupation of the four positions by oxygen or nitrogen donor ligands that are bidentate and that can either be anionic or neutral:

- The bidentate ligand that is more negatively charged is coordinated to equatorial positions  $e_1$  and  $e_2$ , while the remaining ligands coordinate to the one equatorial and the axial positions.
- For a ligand with an NO donor set, the nitrogen atom is coordinated to the equatorial position *cis* to the peroxide oxygen atom. The two oxygen atoms will coordinate to the equatorial position *trans* to the peroxide ligand and to the axial position *trans* to the oxido ligand.<sup>10</sup>

### Diperoxo Complexes

The structural and electronic properties of diperoxo complexes of vanadium have been studied by carrying out *Ab initio* calculations.<sup>9</sup> The geometry that is most likely for the

$[\text{OV}(\text{O}_2)_2]^-$  ion is the one in which the two peroxy groups are parallel to each other depending on the ligand and perpendicular to the oxo oxygen. In this structure, the vanadium atom is raised approximately 0.5 Å out of the plane of the peroxy groups or the equatorial plane in the direction of the vanadyl oxygen atom. The diperoxy complexes of vanadium also show coordination geometry that is distorted pentagonal bipyramidal. The pentagonal plane of the bipyramid is made up of four oxygen atoms from the two peroxy groups (Figure 2) and nitrogen or oxygen from the ligand. The apical position of one of the polyhedron is occupied by oxygen bonded to the vanadium atom by a double bond while the second apical position ( position a in Figure 1) is occupied by either an oxygen or a nitrogen from a ligand.<sup>9,14,15</sup>

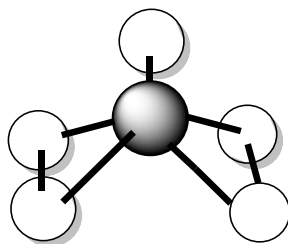


**Figure 2:** Structure of  $[\text{VO}(\text{O}_2)_2]$

### Triperoxo Complexes

Theoretical calculations aimed at elucidating the structure of a triperoxo vanadium complex (Figure 3) reveal that it has a capped trigonal prismatic geometry.<sup>9</sup> But it has no  $\text{V}=\text{O}$  bond as observed in the mono and diperoxo complexes. This also destabilized the triperoxo structure.<sup>9</sup>

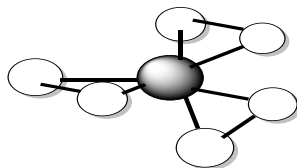


**Figure 3:** Structure of  $[\text{V}(\text{O}_2)_3]$

## Characteristic Spectral Properties of Vanadium Peroxocomplexes

The characteristic spectra for vanadium peroxo complexes show peaks for the groups present in the complex. These groups are V=O, V-O, O-O, and the ligand. In this study, characteristic features of UV-Vis and the IR spectra of some vanadium peroxo complexes will be of interest. These spectroscopic methods are used to make a distinction between the mono-, di-, and triperoxo complexes from their spectra.

### Electron Absorption and UV-Visible Spectroscopy.

The position of the band in the spectrum is influenced both by the solvent and the ligand. Monoperoxido complexes of vanadium(V) compounds that contain the  $\text{VO}(\text{O}_2)^+$  ion in the solid state are red or orange-red in colour. These show an absorption band with a maximum occurring between 400 and 495 nm and a molar absorption coefficient, ranging between 212 to  $420 \text{ mol}^{-1} \text{ dm}^3 \text{ cm}^{-1}$ . The spectrum for the complex  $\text{K}[\text{VO}(\text{O}_2)(\text{OX})(\text{bpy})] \cdot 3\text{H}_2\text{O}$  that was taken in an aqueous solution of  $0.02 \text{ mol/dm}^3$  at  $25^\circ \text{C}$  showed a characteristic band in 400-495 nm range. This band was assigned to the Ligand to Metal Charge Transfer (LMCT) that is interpreted as an electron transfer from the orbitals of the peroxo ligand to the vanadium atomic orbital. Some sources challenge this interpretation by saying the band is not purely LMCT but a combination of LMCT and ligand to ligand transitions. This assertion is justified by quantum chemical calculations. Table 1 shows some monoperoxovanadium(V) complexes and their characteristic bands on the UV-Vis spectrum.<sup>9</sup>

**Table 1:** Electron absorption (UV-Visible region) data for structurally characterized heteroligand monoperoxidovanadium(V) complexes<sup>9</sup>

| Compound   | $\lambda_{\text{max}}$ (nm) [ $\epsilon$ (mol <sup>-1</sup> dm <sup>3</sup> cm <sup>-1</sup> )] |
|--|---|
| [VO(O <sub>2</sub> )(pca)(bpy)]  | 474 [505]   |
| [VO(O <sub>2</sub> )(pca)(phen)]   | 477 [585]   |
| [VO(O <sub>2</sub> )(pic)(H <sub>2</sub> O) <sub>2</sub> ]                     | 450 - 465   |
| [VO(O <sub>2</sub> )(pa) <sub>2</sub> ]ClO <sub>4</sub> ·3H <sub>2</sub> O     | 422 [212]   |
| (NH <sub>4</sub> ) <sub>2</sub> [VO(O <sub>2</sub> )(Hedta)]·4H <sub>2</sub> O | 425   |
| K[VO(O <sub>2</sub> )(omedia)]·H <sub>2</sub> O                                | 439 [357]   |
| K[VO(O <sub>2</sub> )(ox)(bpy)]·3H <sub>2</sub> O                              | 422 [320]   |

In Figure 4, below, is the spectrum of a diperoxo complex. The complex (H<sub>3</sub>O)<sub>2</sub>[V<sub>2</sub>(O)<sub>2</sub>(O<sub>2</sub>)<sub>4</sub>(C<sub>2</sub>H<sub>5</sub>NO<sub>2</sub>)]·5/4H<sub>2</sub>O that has two metal centres is coordinated to two peroxo groups, making the complex a diperoxo vanadium(V) complex. From the spectrum it is observed that (H<sub>3</sub>O)<sub>2</sub>[V<sub>2</sub>(O)<sub>2</sub>(O<sub>2</sub>)<sub>4</sub>(C<sub>2</sub>H<sub>5</sub>NO<sub>2</sub>)]·5/4H<sub>2</sub>O showed a band at 328 nm with an absorption coefficient of 541 M<sup>-1</sup>cm<sup>-1</sup>. The absorbance is also rising into the ultraviolet region. There is also a band at 213 nm with an absorption coefficient of 4257 M<sup>-1</sup>cm<sup>-1</sup>. For this complex, the characteristic ligand to metal charge transfer range is between 320 and 300 nm, which corresponds to the LMCT on the [(V=O)(O<sub>2</sub>)<sub>2</sub>]<sup>-</sup> unit.<sup>16</sup>



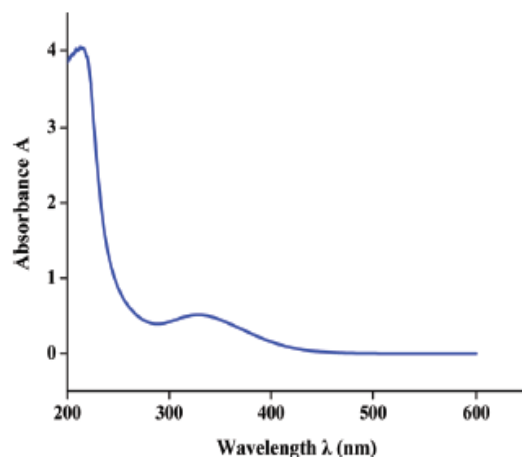


**Figure 4:** UV-Visible spectrum of  $(\text{H}_3\text{O})_2[\text{V}_2(\text{O})_2(\text{O}_2)_4(\text{C}_2\text{H}_5\text{NO}_2)]$  in water<sup>16a</sup>

### FT-IR Spectroscopy

The IR spectra of peroxovanadium complexes usually show absorption bands or peaks corresponding to the oxo and peroxo groups and the ligands attached to vanadium. On the IR spectra, the most important features are  $\nu(\text{V}=\text{O})$ ,  $\nu(\text{O}-\text{O})$ , and also the symmetric and antisymmetric stretching of  $\nu(\text{V}-\text{O}_2)$ . These lie in the regions 930-980, 840-860, and 500-600  $\text{cm}^{-1}$  respectively.<sup>9,12</sup> Figure 5 below is the spectrum of the dark green complex  $[\text{Ni}(\text{NH}_3)_6][\text{VO}(\text{O}_2)_2(\text{NH}_3)]_2$ .<sup>14</sup>

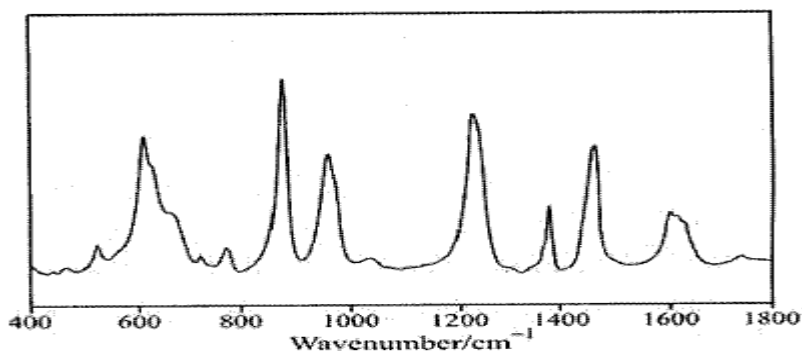


**Figure 5:** IR spectrum of  $[\text{Ni}(\text{NH}_3)_6][\text{VO}(\text{O}_2)_2(\text{NH}_3)]_2$ <sup>20a</sup>

## Vanadium Hydrogen Peroxide Reaction

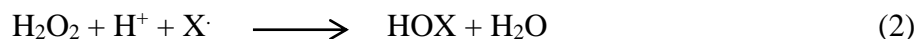
The reactions in systems containing both vanadium salts and hydrogen peroxide are pH and temperature sensitive. The products of such systems depend on the properties of other reagents present, such as their oxidation or reduction potentials. In most cases, the vanadium salts will be oxidized while the peroxide is decomposed.

Vanadate salts react with hydrogen peroxide to produce peroxovanadium complexes of the mono-, di-, and triperoxo species, depending on the molar concentrations of vanadium and hydrogen peroxide present and the pH of the reaction. When the pH of the reacting solution is 1 and the mole ratio of V:H<sub>2</sub>O<sub>2</sub> is 1:2, the product of the reaction will be a monoperoxovanadium(V) complex. When the pH of the reacting medium is about 4 and the H<sub>2</sub>O<sub>2</sub>:V ratio is greater or equal to 3, the product formed is the diperoxo vanadium(V) complex. For the triperoxo complex to be formed, the H<sub>2</sub>O<sub>2</sub>:V ratio should be 5:1 and at a high pH value. All the reactions are carried out at low temperatures between 0 and 5 °C.<sup>12</sup>

A vanadium(IV) complex acts as a catalyst in the oxidation of NAD(P)H by hydrogen peroxide. The reaction pH was 7.4, at a temperature of 25 °C. This reaction proceeds by a free radical chain mechanism in which O<sub>2</sub><sup>-</sup> is the oxidizing agent of NAD(P)H.<sup>17</sup>

## Vanadium Haloperoxidases

Vanadium haloperoxidases (VHPOs) are a group of enzymes found in marine organisms that are responsible for the catalytic oxidation of halide ions by hydrogen peroxide.<sup>17</sup> The products of the oxidation are the corresponding hypohalous acids. These enzymes are also capable of halogenating organic substrates.



The enzymes are named based on their ability to oxidize halides. Chloroperoxidase oxidizes chlorides, bromides, and iodides. Bromoperoxidases do not oxidize chlorides, while iodooxidases oxidize only iodides. A variety of organic substrates are halogenated and also dimerized by VHPOs while thioethers are oxygenated to sulfoxides.

X-ray diffraction studies on VCiPO from the pathogenic fungus *Curvularia inaequalis* provide information on the structural features of the inorganic cofactor and its environment. This study reveals that the vanadium ion has a trigonal bipyramidal geometry Figure 6.<sup>18</sup> In this geometry, three oxygen atoms are in the equatorial plane while one is on the axial position. His496 is an apical ligand and links the metal ion to the protein. The oxygen atoms form hydrogen bonds with amino acids such as Lys353, Arg360, His404, and Arg490. The first and second coordination spheres of the cofactor are well conserved across species as revealed from crystallographic studies.<sup>18</sup>

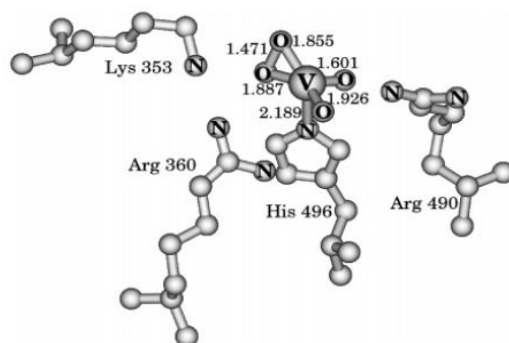


**Figure 6:** Structure of the active side of vanadium containing haloperoxidase<sup>18a</sup>

Investigations on the catalytic properties of VHPOs show that vanadium remains in the V oxidation state throughout the catalytic cycle.<sup>18</sup> The vanadium metal serves as a strong Lewis

acid in the activation of the primary oxidant,  $\text{H}_2\text{O}_2$ . It was also observed that the amino acid Lys353 that interacts directly with the peroxo-bound moiety may polarize the peroxo bond and make it more susceptible towards nucleophilic attack. It has also been proven that the hypohalous acid product is a functional, site-selective halogenating agent. Its site-selective halogenating properties can either be harnessed as is or as in special cases of iodide and bromide, as  $\text{X}_3^-$ .<sup>18</sup>

Studies carried out on synthetic peroxo-vanadium complexes show that the rate of halide oxidation generally increases with the addition of acids.<sup>18</sup> Spectroscopic data reveal that the reaction progresses with the protonation of one or more sites on the complex. This suggests that cleavage of the heterolytic peroxide, O-O, bond could be assisted by a side-on bound hydroperoxide. Despite numerous studies and the massively investigated VHPOs models, the synthesis of models that are identical to the metal coordination environment observed in the enzyme has not been achieved. This limits the comparison of chemical properties of models with that of the active site in the enzyme. It has not been clearly established whether protonating the peroxo group is a prerequisite for activation in the enzyme. If this is the case, which of the oxygen sites does the halide attack, the protonated or the unprotonated oxygen? In addition, x-ray structures obtained for the peroxo derivative of VHPO reveal a potentially vacant coordination site. This leads to the observation that halides bind to the vanadium prior to oxidation. It is also not known which of the oxygens is involved in the oxo-transfer. That is, is it the pseudo axial or the equatorial peroxo oxygen atom that is involved in the oxo-transfer?<sup>18</sup> These enzymes are thought to be involved in the biosynthesis of a large number of marine natural products with potential antifungal, antibacterial, antiviral, and antineoplastic properties.<sup>18</sup>

These above mentioned questions that are unanswered about the enzyme system, in addition to the fact that vanadium complexes catalyze a wide variety of organic reactions, are the reasons why this work is set to carry out studies on the vanadiumoxoperoxo system. This is to contribute to the efforts that are being put forward to help understand both the structure and the mechanism of the catalytic reactions of VHPO. With such knowledge, a mimic of the VHPO active site in the lab will generate the ideal catalyst for halide oxidation in addition to many other reactions. It should also be mentioned that organic halides are intermediates in many organic syntheses. If an ideal catalyst can be generated for the halogenation reactions, then many organic syntheses will be a lot easier than they are at present.

#### Goals for this Research

This work is part of the ongoing research of the Wardeska research group that is geared towards understanding the synthesis, structures, and mechanisms of catalytic reactions and reaction conditions of the vanadium oxoperoxo complexes. In a previous study, Hima Patel investigated “The Effect of pH on the Reaction Between [VOHEDTA]<sup>-1</sup> and Hydrogen Peroxide Using Electron Absorption Spectroscopy”.<sup>20</sup> According to this study, it was established that the reaction is pH sensitive. The reaction was faster at low pH values below pH 3 and below.<sup>20</sup>

In another study, Brandon Paul Maye investigated “An Analysis of the Peroxidation of Vanadium Hydroxyethylethylenediaminetriacetic Acid”. In his study, it was confirmed that the hydroxyl arm and one carboxylic acid group on HEDTA condensed to form a lactone ring in the vanadium oxoperoxo complex to form a molecule designated omedia. The omedia binds to the vanadium oxoperoxo moiety by forming a chelate while coordinating by the two amines and the two deprotonated carboxylate arms of HEDTA.<sup>21</sup> Elaina Campbell, on her part, worked on the

kinetics of the reaction between  $[\text{VOHEDTA}]^{-1}$  and  $\text{H}_2\text{O}_2$ .<sup>22</sup> She found that the reaction is first order with respect to  $[\text{VOHEDTA}]^{-1}$  and  $\text{H}_2\text{O}_2$  concentrations and a half order with respect to the acid concentration.<sup>22</sup>

Studies on the reaction of vanadium compounds with hydrogen peroxide and HEDTA had been part of the research work in the Wardeska group. Other areas of research in this group involves forming complexes with copper with a variety of ligands one of which was a Schiff base that was synthesized as part of research work in the group.

The ultimate ambition of this work was to synthesize and characterize the compounds containing  $[\text{VO}(\text{O}_2)\text{HEDTA}]^{-2}$ . In this research, gains were made by preparing and characterizing  $[\text{VO}(\text{O}_2)\text{H}_2\text{EDTA}]^{-2}$  and also investigating its ability to catalyze oxibromination. The reaction between  $[\text{VOHEDTA}]^{-1}$  and hydrogen peroxide was also studied. These goals were achieved by the accomplishment of the following;

- Prepare a solution of  $[\text{VOHEDTA}]^{-1}$ .
- Prepare a solution of  $[\text{VO}(\text{O}_2)\text{HEDTA}]^{-2}$ .
- Study the effect of acid on the  $[\text{VO}(\text{O}_2)\text{HEDTA}]^{-2}$  in solution.
- Determine the rate equation for the reaction of  $[\text{VO}(\text{O}_2)\text{HEDTA}]^{-2}$  and acid and propose a mechanism consistent with the equation.
- Isolate and characterize  $[\text{VO}(\text{O}_2)\text{H}_2\text{EDTA}]$  as a solid.
- Test the catalytic properties of  $[\text{VO}(\text{O}_2)\text{H}_2\text{EDTA}]$ .
- Synthesize a V(V) oxoperoxo complex from a V(IV) compound.

## CHAPTER 2

### METHODOLOGY

#### Materials and Reagents

##### Reagents

Research grade vanadium(IV) sulfate,  $\text{VOSO}_4 \cdot 5\text{H}_2\text{O}$ , (18.5% V), was purchased from Johnson Matthey Electronics and was used with no further purification. Research grade barium perchlorate ( $\text{Ba}(\text{ClO}_4)_2 \cdot 3\text{H}_2\text{O}$ ) and  $\text{KNO}_3$  were purchased from G. Frederick Smith Chemical Company and were used without further purification. Research quality hydrogen peroxide, 30%, calcium chloride, potassium hydroxide, sodium hydroxide, perchloric acid, salicylaldehyde, potassium permanganate, were purchased from Fisher Scientific Chemical. Research quality sodium oxalate powder primary standard was purchased from J. T. Baker Chemical Co. Potassium bromide, FTIR grade, was purchased from Alfa Aesar, A Johnson Mathy Company. Research grade ethyl alcohol was purchased from AAPER Alcohol and Chemical Co. and was used as purchased. The deionized water was produced using Water Professional Instrument. Buffer solutions of pH 4 and 7 were from Fisher Scientific.

##### Materials

The pH of the solutions was measured using a Fisher Accumet Model 925 pH meter produced by Fisher Scientific. It had a pH measurement with resolution of 0.001 in pH units. It had a one- to five- point standardization. The Fisher Accumet Model 925 pH meter was used in combination with a Fisher combination electrode. The combination electrode had both the reference and measuring electrode combined in a single housing. It is made up of a pH indicating electrode coaxially joined to a silver/silver chloride reference electrode. The indicating glass pH

electrode was at the center of the probe. The outer space contained a silver/silver chloride reference electrolyte, which was a 4 M KCl solution saturated with AgCl, and a porous plug junction. When immersed in a solution, contact (between the reference electrode and pH indicating and sample electrode) was made through the porous plug junction. The pH meter was calibrated with a buffer solution of pH 4 or 7 each time before use.

The weighed samples were measured with a Mettler Toledo model PB403 electronic top pan mass balance. It measures to 0.001 of a gram. Vacuum filtration and drying were accomplished with a KNF Neuberger, INC vacuum pump model UN726FTP. Fourier transform infrared spectrometry analysis was done with a Genesis II FTIR spectrometer produced by Mattson Instruments. The instrument was controlled by a WinFIRST software from the same company. The instrument is equipped with an Infrared Ceramic Emitter (ICE) as the infrared source, lithium tantalite ( $\text{LiTaO}_3$ ) type detector, helium-neon (HeNe) laser as the monochromatic light source. Stirring was done with a magnetic stirrer and a bar magnet. The magnetic stirrer was an Isompt that has a hot plate and a stirrer in one produced by Fisher Scientific. The UV-Visible studies were done with a Pharmaspec UV-1700 series spectrophotometer produced by Shimadzu Corporation. Ordinary laboratory glassware was used for most of the routine measurements and manipulations. Gas chromatography mass spectroscopy (GC-MS) experiments were done with a Hewlett Packard instrument. The instrument is made up of three components, a 5971 Series Mass Selective Detector, a 5890 Series II Gas Chromatograph, and 59822B Ionization Gauge Controller. Elemental analysis of samples was done by Galbraith Laboratories, Inc. Carbon, hydrogen, and nitrogen analysis were done by combustion analysis,

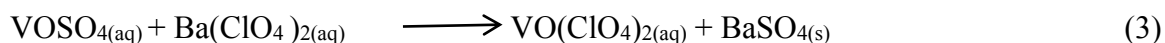


while vanadium was analyzed by Inductively Coupled Plasma Optical Emission Spectroscopy (ICP-OES).

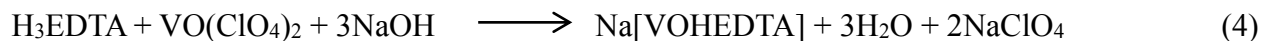
### Preparation of Solutions and Complexes

#### Preparation of [VOHEDTA]<sup>-1</sup> Solution

The [VOHEDTA]<sup>-1</sup> solution was prepared from a solution of VO(ClO<sub>4</sub>)<sub>2</sub> and H<sub>3</sub>EDTA. The VO(ClO<sub>4</sub>)<sub>2</sub> solution was prepared by mixing solutions of vanadium(IV) sulfate and barium perchlorate. The VOSO<sub>4</sub> solution was prepared by dissolving 2.533 g of VOSO<sub>4</sub>·5H<sub>2</sub>O (0.01000 mmol) in 20.0 mL of distilled water. The Ba(ClO<sub>4</sub>)<sub>2</sub> solution was prepared by weighing and dissolving 3.903 g (0.01000 mmol) of Ba(ClO<sub>4</sub>)<sub>2</sub> in 25.0 mL of distilled water. The two solutions were then mixed together, which formed insoluble BaSO<sub>4</sub>, a white precipitate, and a blue VO(ClO<sub>4</sub>)<sub>2</sub> solution.



The fine white insoluble BaSO<sub>4</sub> was removed by suction filtration using a fine glass frit. The VO(ClO<sub>4</sub>)<sub>2</sub> filtrate was transferred to a 100 mL volumetric flask and distilled water was added to the 100 mL mark. The solution was standardized by titration with a stock solution of 0.0104 M KMnO<sub>4</sub> (see Appendix A). The absorption spectrum of the solution was recorded and the molar extinction coefficient (ε) was calculated from Beer's law. The mass of H<sub>3</sub>EDTA, 0.137 g (0.500 mmol), was weighed into a beaker and 5 mL of distilled water was added sodium hydroxide. 1.5 mL of 1.0 M NaOH (1.5 mmol) was added to the beaker and the mixture was stirred until all the H<sub>3</sub>EDTA had dissolved, and 4.92 mL (0.5 mmol) of VO(ClO<sub>4</sub>)<sub>2</sub> solution was measured in to the beaker.



Potassium nitrate, 2.5 mL of 1.0 M was added to give an ionic strength of 0.10 M. Distilled water was then added to the mixture to make the volume total 25 mL. The pH of the solution was adjusted to 3.12 by adding 2.0 M KOH and 1.0 M HClO<sub>4</sub>. The UV-Visible spectrum of the solution was recorded and used to determine the exact concentration by the Beer-Lambert law.

#### Reaction of [VOHEDTA]<sup>-1</sup> with H<sub>2</sub>O<sub>2</sub>

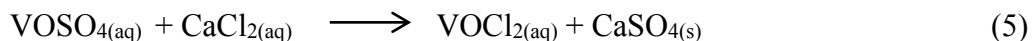
To the solution prepared ([VOHEDTA]<sup>-1</sup>), 0.8 mL (0.776 mmol) of 3% hydrogen peroxide (H<sub>2</sub>O<sub>2</sub>) previously prepared from a 30% stock solution was added. The progress of the reaction was monitored with a UV-Visible spectrometer. The reaction lasted for about 42 minutes (2500 s).

#### Initial Rate Study of the Effect of [H<sup>+</sup>] on the Decomposition of [VO(O<sub>2</sub>)HEDTA]<sup>-2</sup> in Solution

Four aliquots of 1.00 mL (0.020 mmol) of the [VO(O<sub>2</sub>)HEDTA]<sup>-2</sup> solution were measured into separate beakers with a syringe. To each of the four sections was added 4.5 mL (4.5 mmol), 5.0 mL (5.0 mmol), 6.0 mL (6.0 mmol), and 6.5 mL (6.5 mmol) of 1.0 M HClO<sub>4</sub> acid. The reaction was monitored with a UV-Visible spectrometer over a period of 35 minutes (2100 s). The reactions were tested for zero, half, first, and second orders.

#### Synthesis of [VO(O<sub>2</sub>)H<sub>2</sub>EDTA]

A solution of VOSO<sub>4</sub> was prepared by weighing and dissolving 1.5 g (0.0060 mol) VOSO<sub>4</sub>·5H<sub>2</sub>O in 20 mL of distilled water and then mixing it with a solution of CaCl<sub>2</sub> prepared by weighing and dissolving 0.7 g (0.006 mol) CaCl<sub>2</sub> in 10 mL distilled water. The reaction solution was allowed to stand overnight.



A white precipitate of  $\text{CaSO}_4$  was formed. The white precipitate was removed by filtration. The solution was evaporated to half of its volume by mild heating, while stirring. The concentrated solution was allowed to cool to room temperature, then it was placed in an ice bath. Hydrogen peroxide, 30%, 1.20 mL (11.640 mmol) was measured and added to the solution while stirring in an ice bath. A mass of 1.670 g (6.000 mmol) of  $\text{H}_3\text{EDTA}$  was weighed and added to the reaction mixture while the mixture was stirred. The stirring was continued until all the  $\text{H}_3\text{EDTA}$  had dissolved. The pH was measured to be 1.658. The solution was stirred for a couple of hours in an ice bath, after which it was allowed to stand at room temperature for two days. A yellow precipitate formed which was filtered, washed with distilled water, and allowed to dry on the vacuum filter. The precipitate was analyzed by FT-IR and UV-Vis. Elemental analysis of the precipitate found: %C, 34.93; %H, 4.41; %N, 7.71; %V, 13.3, and %O, 39.65 for the formula  $\text{VO}(\text{O}_2)\text{C}_{10}\text{H}_{17}\text{N}_2\text{O}_7$ . The calculated percentage composition is %C, 31.93; %H, 4.56; %N, 7.45; %V, 13.54, and %O, 42.52.

#### Test for the Catalytic Properties of $[\text{VO}(\text{O}_2)\text{H}_2\text{EDTA}]$

The catalytic ability of the complex was examined by carrying out an oxidative bromination reaction on salicylaldehyde.<sup>22</sup> The reaction temperature was 50 °C with a volume of 20 mL of distilled water. Four portions each of 0.001 g catalyst ( $2 \times 10^{-3}$  mmol), 0.132 mL (1.43 mmol) salicylaldehyde, 0.295 g (2.50 mmol) KBr, 0.26 mL (2.5 mmol) of 30%  $\text{H}_2\text{O}_2$ , and 0.21 mL (2.5 mmol) of 70%  $\text{HClO}_4$  were added to the mixture in distilled water while stirring under reflux in a time interval of 30 min. The portions were added at 30 min, 60 min, 90 min, and 120 min. At the end of the reaction, a total of 0.004 g catalyst, 0.528 mL salicylaldehyde, 1.18 g KBr, 1.04 mL 30%  $\text{H}_2\text{O}_2$  and 0.84 mL of 70%  $\text{HClO}_4$  were reacted. At the end of the reaction, 10 mL

of  $\text{CH}_2\text{Cl}_2$  was added to the mixture. The mixture was then transferred to a separatory funnel. The organic layer was separated from the aqueous layer and then returned to the funnel and washed with a large volume of distilled water. The product was then allowed to stand in the hood under mild heating at about  $50\text{ }^\circ\text{C}$  to evaporate the  $\text{CH}_2\text{Cl}_2$ . The product was analyzed by GC-MS.<sup>23</sup> The sample for analysis by GC-MS was prepared by mixing  $20\text{ }\mu\text{L}$  of the product in  $2\text{ mL}$  of acetone. A total of four reactions were done, two of them had the catalyst while two had no catalyst. Two of the reactions were done with the acid while two others had no acid.

#### Electronic Absorption and UV-Visible Studies

The UV-Visible studies were done by placing a portion of the solution in a sample quartz cuvet and a reference solution in the reference cuvet. The cuvetts were  $1\text{ cm}$  in length. For the  $\text{VO}(\text{ClO}_4)_2$  spectrum the  $\text{VO}(\text{ClO}_4)_2$  solution was in the sample cuvet while distilled water was in the reference cell. For all the other studies, a volume of the solution was in the sample cuvet while a solution of  $1.0\text{ M KNO}_3$  was in the reference cell. For UV-Visible studies of the catalyst, the catalyst was dissolved in dimethylsulfoxide (DMSO), and the reference cuvette contained DMSO.

#### Gas Chromatography Mass Spectrometry Studies

The GC-MS instrument had a low mass of  $50\text{ amu}$ , a high mass of  $550\text{ amu}$ , and a solvent delay time of  $3\text{ minutes}$ . The initial oven temperature,  $70\text{ }^\circ\text{C}$ , was held for  $2\text{ minutes}$  and ramped to  $280\text{ }^\circ\text{C}$  at a rate of  $20\text{ }^\circ\text{C}/\text{min}$ . The total run time was  $15.50\text{ min}$ , the injector temperature was  $250\text{ }^\circ\text{C}$ , the detector temperature was  $280\text{ }^\circ\text{C}$ , the oven equilibrium time was  $0.50\text{ min}$ , and the injection volume was  $1\text{ }\mu\text{L}$ .

## Fourier Transform Infrared Spectroscopy Studies

The FT-IR samples were analyzed as KBr pellets. A KBr pellet was produced by crushing IR grade KBr in a mortar with a pestle. The powder was transferred to the pellet apparatus between two flat polished surfaces. This was mounted on a hydraulic press and kept under pressure of 10 KPa for about 10 minutes. The KBr pellet was scanned as back ground. For the sample scan, the pellet was prepared by grinding a small portion of the sample in KBr and the procedure was repeated as above.

## CHAPTER 3

### RESULTS

#### Preparation of Solutions and Complexes

The UV-Visible absorption spectrum of a 0.100 M  $\text{VO}(\text{ClO}_4)_2$  solution showed a single intense absorption band at 764 nm ( $A = 1.6416$ ) with a second band observed as a shoulder around 650 nm, which is a d-d transition (see Figure 7). This absorption band corresponds to the absorption of V(IV) metal ion. The solution had the characteristic blue color of a vanadium(IV) oxidation state ion.<sup>24,29</sup>

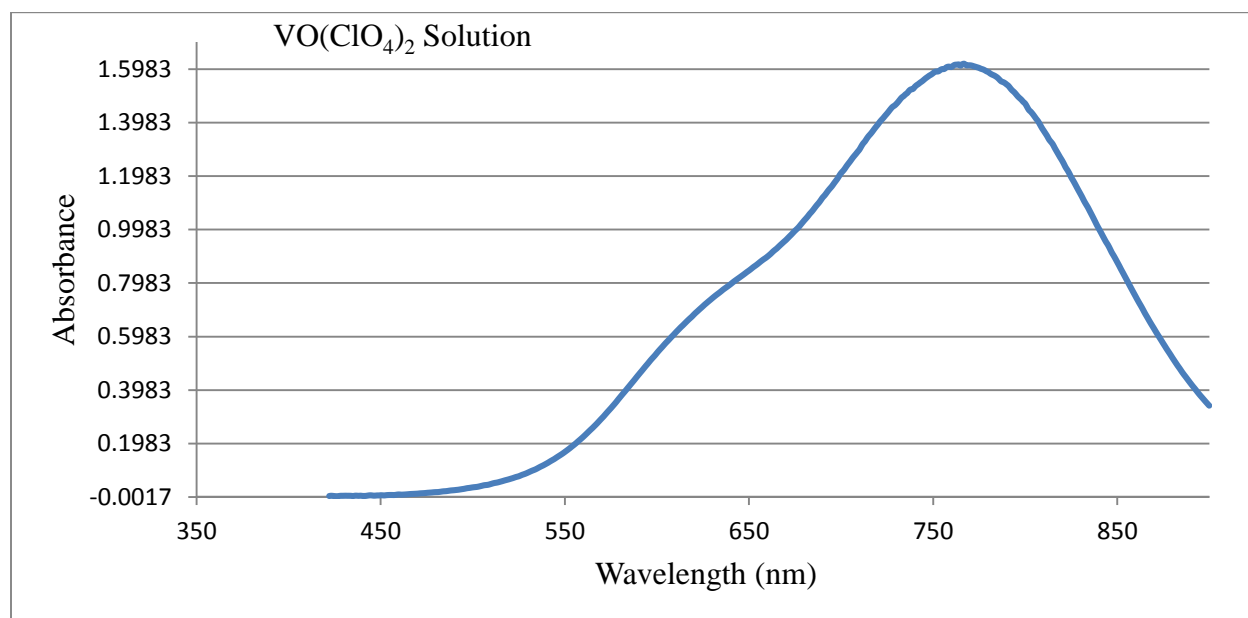


**Figure 7:** The UV-Visible spectrum of  $\text{VO}(\text{ClO}_4)_2$  solution

From the Beer-Lambert law,  $A = \epsilon LC$

where, A = absorbance, L = length of cuvet, C = concentration of solution, and  $\epsilon$  = molar extinction coefficient. Using the Beer-Lambert Law,  $\epsilon = A/LC = 1.7056/1 \text{ cm} \times 0.100 \text{ M} = 15.97 \text{ cm}^{-1}\text{M}^{-1}$ . The pH of the solution was measured to be 2.139. The molar extinction coefficient value agrees with reference which is  $16.00 \text{ cm}^{-1}\text{M}^{-1}$ .<sup>24</sup>

The absorption spectrum of  $0.020 \text{ M } [\text{VO}(\text{HEDTA})]^{-1}$  solution showed two absorption bands. The absorption band at 775 nm has an absorbance of 0.4512 while the absorption band at 585 nm has an absorbance of 0.3761. The molar extinction coefficient for the band at 775 for  $[\text{VO}(\text{HEDTA})]^{-1}$  was calculated as  $21.12 \text{ cm}^{-1}\text{dm}^3\text{mol}^{-1}$ , see Figure 8.

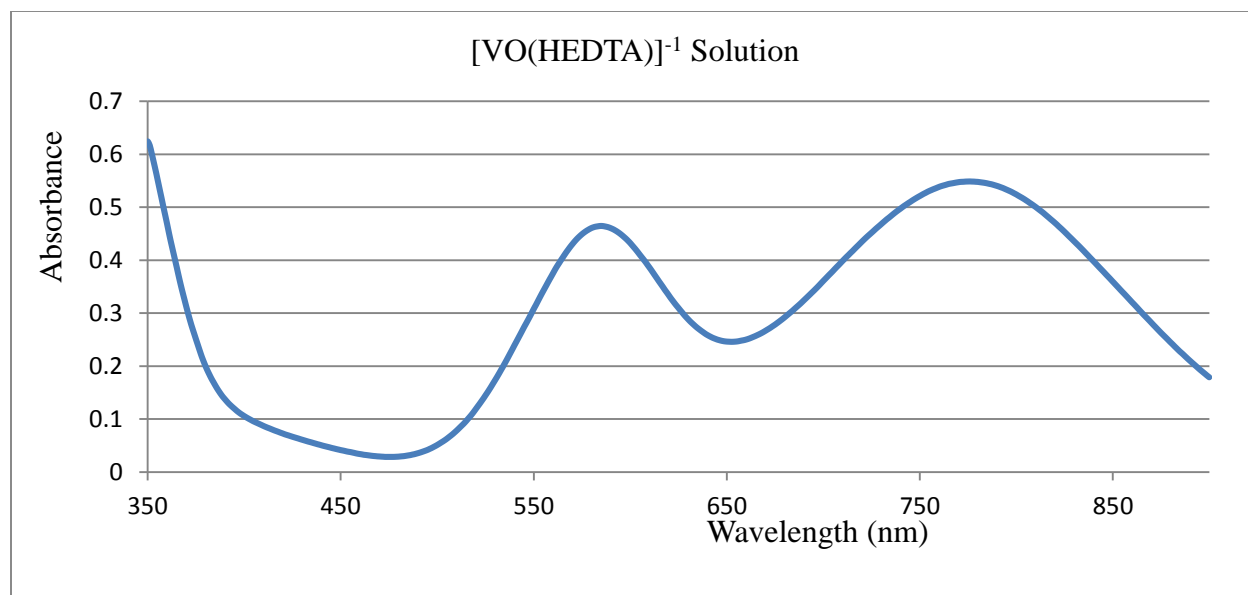


**Figure 8:** The UV-Visible spectrum of  $[\text{VO}(\text{HEDTA})]^{-1}$  solution

The two bands for both  $\text{VO}(\text{ClO}_4)_2$  and the  $[\text{VO}(\text{HEDTA})]^{-1}$  solutions are d-d transitions of V(IV) which is a  $d^1$  ion. In an octahedral ion there should be a single  ${}^2T_{2g} \rightarrow {}^2E_g$  transition; however, the symmetry in these ions is less than octahedral, so the energy level splits, giving two

transitions; for  $[\text{VO}(\text{HEDTA})]^{-1}$ , is assigned to the 775 nm ( $12,900 \text{ cm}^{-1}$ ) as a  ${}^2\text{B}_{2(xy)} \rightarrow {}^2\text{E}_{(xz,yz)}$  transition, and one near 586 nm ( $15,900 \text{ cm}^{-1}$ ) is the  ${}^2\text{B}_{(xy)} \rightarrow {}^2\text{B}_{(x^2-y^2)}$  transition, assuming an approximate  $\text{C}_{4v}$  symmetry.<sup>25,29</sup>

### Spectrum For The Reaction Between $[\text{VO}(\text{HEDTA})]^{-1}$ and $\text{H}_2\text{O}_2$

The reaction between  $[\text{VO}(\text{HEDTA})]^{-1}$  and  $\text{H}_2\text{O}_2$  progressed smoothly as anticipated. The intensity of the absorption band at 775 nm decreased over the course of the reaction, while a new absorption band formed at 425 nm. The absorption band at 580 nm did not show any increase or a decrease, but an isosbestic point was formed near that point, see Figure 9.

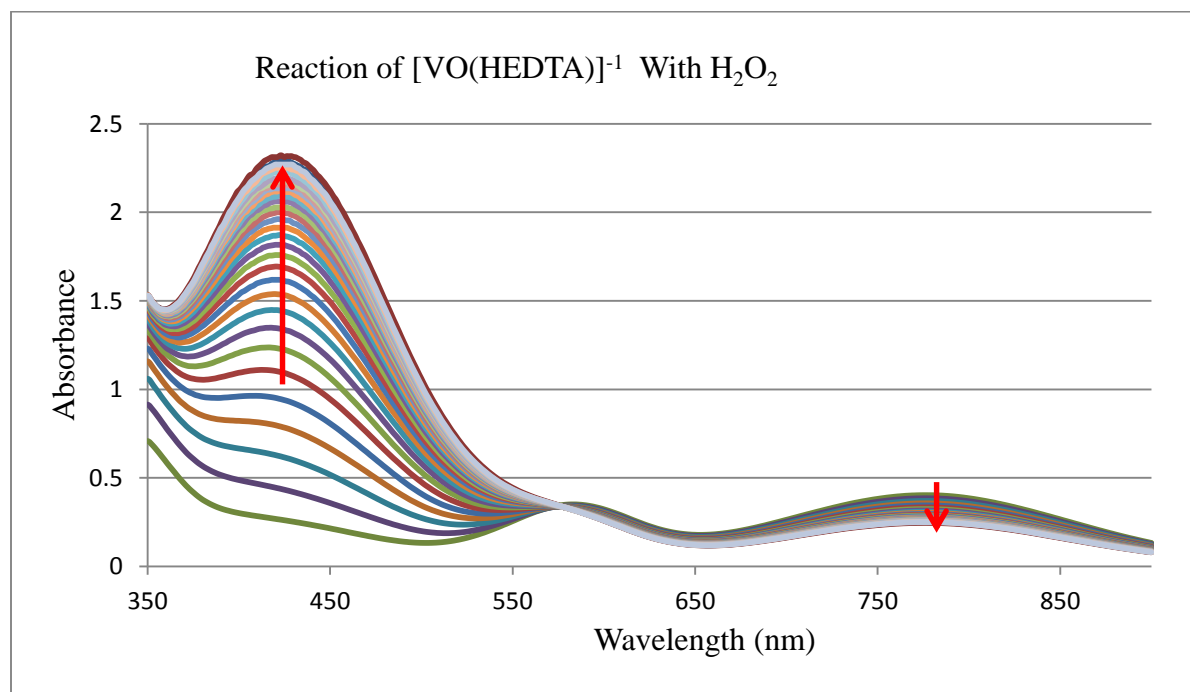


**Figure 9:** The UV-Visible spectrum for the reaction between  $[\text{VO}(\text{HEDTA})]^{-1}$  (0.02136 M) and  $\text{H}_2\text{O}_2$  (0.97 M) showing the progress of the reaction with time



The decrease in intensity of the absorption band at 775 nm is as a result of the oxidation of the vanadium(IV) into the vanadium(V) metal ion. As more of the metal is oxidized, the intensity of the band decreases with decreasing concentration of the absorbing species. The new absorption band at 425 nm is a due to the LMCT absorbance band of the vanadium(V) oxoperoxo moiety.<sup>10</sup> The absorbance increases as the concentration of the moiety increases in the solution. The isosbestic point was observed at about 585 nm, which indicates that there were no intermediate or side reactions in the reaction. At the end of the reaction, not all the vanadium(IV) is oxidized to the vanadium(V) oxidation state. This may be seen from the presence of the absorption band at 775 nm. The band at 775 nm does not disappear or level off but still shows an absorbance of 0.2465. The new band at 425 nm shows a maximum absorbance of 2.9368. The reaction lasted for a period of about 41minutes (2460 seconds), see Figure 10.

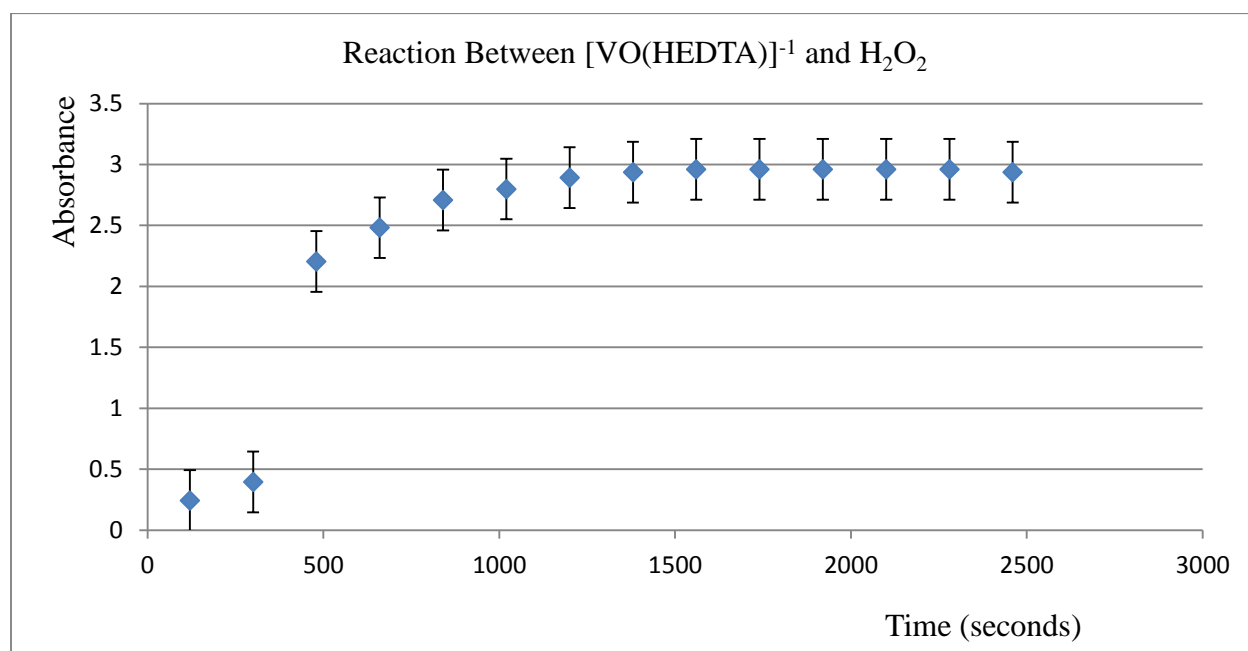


**Figure 10:** A plot of the absorbance at 425 nm against time for the reaction between  $[\text{VO}(\text{HEDTA})]^{-1}$  and  $\text{H}_2\text{O}_2$

Knowing the volumes and concentrations used in the experiment and assuming a 1:1 correspondence between reactant and product, it is possible to use the spectral changes from Figure 10 to calculate the  $\epsilon_{425}$  for the oxoperoxo product. The mmol of  $[\text{VOHEDTA}]^{-1}$  may be calculated; volume of  $[\text{VOHEDTA}]^{-1}$  solution = 25.0 mL, concentration of  $[\text{VOHEDTA}]^{-1} = 0.5$  mmol/25.0 mL = 0.02136 M, From Beer's law,  $A = \epsilon LC$ ,  $\epsilon_{775} = 0.4512/(1 \text{ cm} \times 0.02136) = 21.12 \text{ cm}^{-1}\text{dm}^3\text{mol}^{-1}$ ,  $\Delta A_{775} = \epsilon L \Delta C$ ,  $\Delta C = \Delta A_{775}/\epsilon L$ ,  $\Delta A_{775} = A_i$  (before reaction with  $\text{H}_2\text{O}_2$ ) –  $A_f$  (at the end of reaction with  $\text{H}_2\text{O}_2$ ). So,  $\Delta A_{775} = 0.4512 - 0.2773 = 0.1739$ ,  $\Delta C[\text{VOHEDTA}]^{-1} = 0.1739/(21.12 \text{ cm}^{-1}\text{M}^{-1} \times 1\text{cm}^{-1}) = 0.0082 \text{ M}$ . Assuming the change in concentration at 775 nm was the same as the increase in concentration at 425 nm (see Figure 11), then  $\epsilon_{425} = 1.8755/(0.0082 \text{ M} \times 1 \text{ cm}) = 227.78 \text{ cm}^{-1}\text{M}^{-1}$

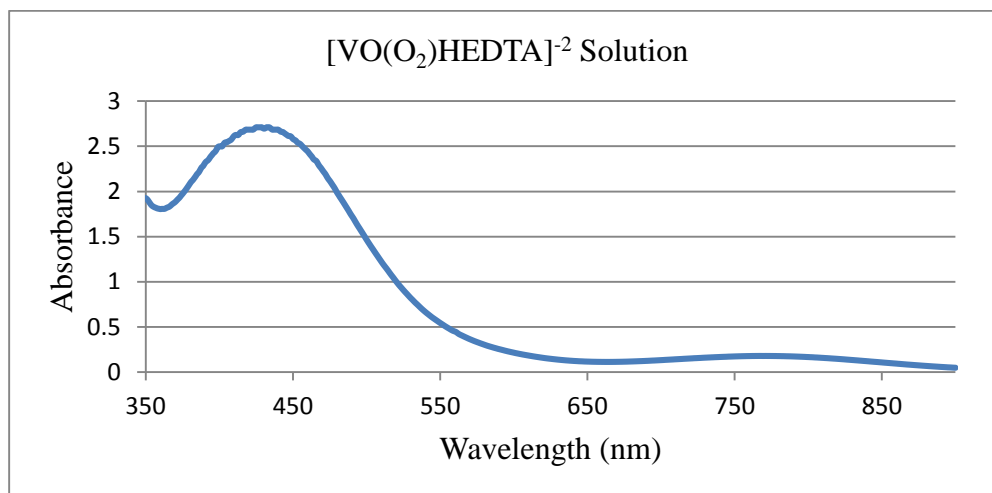


**Figure 11:** The UV-Visible spectrum of  $[\text{VO}(\text{O}_2)\text{HEDTA}]^{-2}$  solution

The reaction between  $[\text{VO}(\text{HEDTA})]^{-1}$  and hydrogen peroxide is expected to produce the oxoperoxo complex  $[\text{VO}(\text{O}_2)(\text{HEDTA})]^{-2}$ .<sup>9</sup> From the literature, the vanadium oxoperoxo moiety should have a molar extinction coefficient between 212 and 420  $\text{mol}^{-1} \text{ dm}^3$

$\text{cm}^{-1}$  and an absorption band between 400 and 495 nm.<sup>9</sup> From the absorption spectrum of the reaction as seen above there is an absorption band at 425 nm with a molar extinction coefficient of  $227.78 \text{ cm}^{-1}\text{dm}^3\text{mol}^{-1}$ . These values fall within the range as expected for the vanadium(V) oxoperoxo moiety.<sup>9</sup>

#### Initial Rate Studies of the Effect of $[\text{H}^+]$ on $[\text{VO}(\text{O}_2)\text{HEDTA}]^{-2}$ in Solution

##### A Fixed Concentration of $[\text{VO}(\text{O}_2)\text{HEDTA}]^{-2}$ in Solution while the Concentration of Acid is Varied

Four 1.00 mL aliquots (0.023 mmol) of  $[\text{VO}(\text{O}_2)\text{HEDTA}]^{-2}$  solution were transferred into beakers with a syringe and reacted with four volumes: 4.5 mL (4.5 mmol), 5.0 mL (5.0 mmol), 6.0 mL (6.0 mmol), 6.5 mL (6.5 mmol) of 1.0 M  $\text{HClO}_4$  acid. The four reactions were studied with a UV-Vis spectrometer (see Figure 12). The reaction between  $[\text{VOHEDTA}]^{-1}$  and  $\text{H}_2\text{O}_2$  was pH sensitive, as the reaction was faster with decreasing pH. The time for the decrease in absorbance at 425 nm was plotted against concentration for each of the four mixtures.

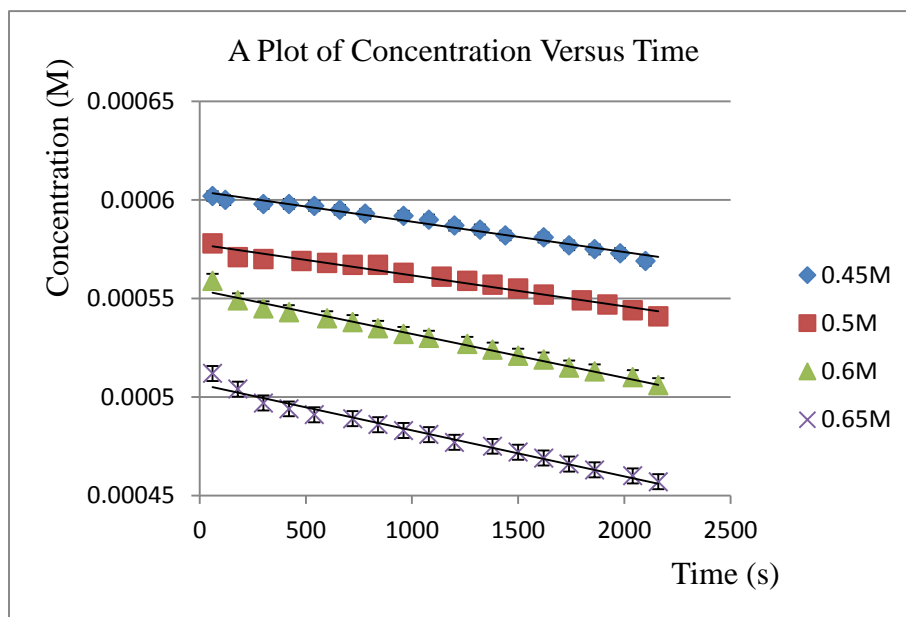


**Figure 12:** A plot of concentration against time in seconds versus concentrations of acid

The reaction was observed over a period of 35 minutes. The decrease in absorbance was attributed to the decomposition of the  $[\text{VO}(\text{O}_2)\text{HEDTA}]^{-2}$  complex. The order of the decomposition reaction with respect to  $[\text{H}^+]$  was calculated as presented in Table 2 and Figure 13.

**Table 2:** Volume of Acid, Concentration of  $[\text{H}^+]$  and Initial Rates

| Volume of Acid | $[\text{H}^+]$ | Initial rate (M/s)    | $R^2$  |
|----------------|----------------|-----------------------|--------|
| 4.5 mL         | 0.45 M         | $1.55 \times 10^{-8}$ | 0.9763 |
| 5.0 mL         | 0.50 M         | $1.59 \times 10^{-8}$ | 0.9737 |
| 6.0 mL         | 0.60 M         | $2.31 \times 10^{-8}$ | 0.9847 |
| 6.5 mL         | 0.65 M         | $2.34 \times 10^{-8}$ | 0.9797 |

In order to determine the order of the reaction by initial rates, the slopes of the lines from Figure 12 were plotted against acid concentration for the various volumes of acid. The plot was linear for all four volumes of acid. This implies that the reaction of decomposition of

$[\text{VO}(\text{O}_2)\text{HEDTA}]^{-2}$  was first order with respect to the concentration of the acid, as shown by a higher  $R^2$  value (0.9260) for first order than for zero (# N/A), half (0.9256) or second (0.9235) orders.

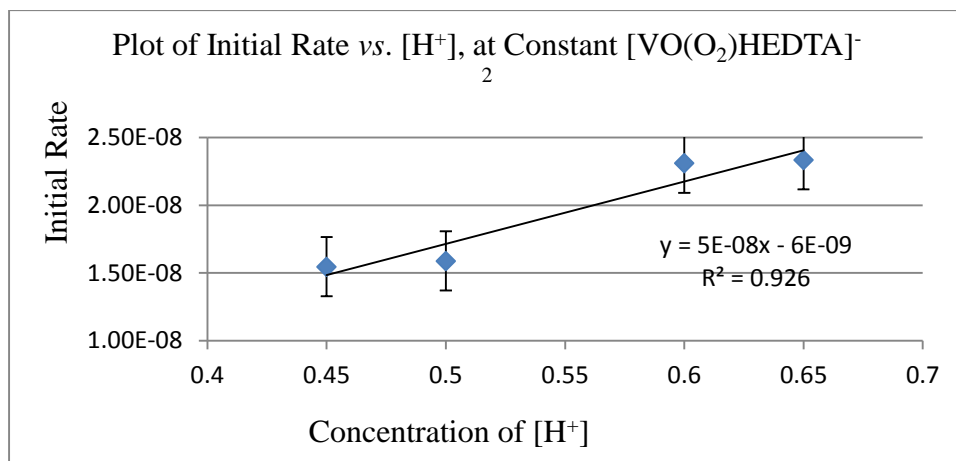


**Figure 13:** Plot of initial rates against concentration of  $[\text{H}^+]$  for the various aliquots of acid

The total volume of reaction system was 25.0 mL by dilution of 5.0 mL of 0.1 M  $[\text{VOHEDTA}]^{-1}$ . The following calculations were to determine the concentrations of various species in the reaction.

$$5.0 \text{ mL} \times 0.1068 \text{ mmol/mL } [\text{VOHEDTA}]^{-1} = 0.534 \text{ mmol/25.0 mL} = 0.02136 \text{ M}$$

$$(1.0 \text{ mL} \times 0.02136 \text{ M})/10 \text{ mL} = 2.136 \times 10^{-3} \text{ M}$$

$$\text{H}_2\text{O}_2 \Rightarrow (2.50 \text{ mL})/25.0 \text{ mL} = (2.50 \text{ mL}/25.0 \text{ mL}) \times 9.71 \text{ M} = 0.97 \text{ M}$$

$$0.50 \text{ mL of 3\% H}_2\text{O}_2 = 0.50 \text{ mL} \times 0.97 \text{ M} = 0.485 \text{ mmol/25.0 mL} = 0.0194 \text{ M}$$

$$\Rightarrow [\text{VOHEDTA}]^{-1} = 0.002136 \text{ M}$$

$$\Rightarrow [\text{VO}(\text{O}_2)\text{HEDTA}]^{-2} = 0.002136 \text{ M}$$

$$k_{\text{obs}} = k[\text{VO}(\text{O}_2)\text{HEDTA}]^{-2} = 4.598 \times 10^{-8}$$

$$\Rightarrow k = 4.589 \times 10^{-8} / 0.002136 = 2.15 \times 10^{-5} \text{ s}^{-1} \text{ M}^{-1} \quad R^2 = 0.9252$$

A Fixed Concentration of Acid While Concentration of  $[\text{VO}(\text{O}_2)\text{HEDTA}]^{-2}$  in Solution is Varied

Four aliquots of 5.0 mL (1 mmol) 1.0 M  $\text{HClO}_4$  were pipetted in to different beakers and reacted with 1.0 mL (0.02 mmol), 1.5 mL (0.03 mmol), 2.5 mL (0.05 mmol), and 3.50 mL (0.07 mmol) of  $[\text{VO}(\text{O}_2)\text{HEDTA}]^{-2}$  solution. The reaction was observed for a period of 35 minutes with a UV-Vis spectrometer and the results were analysed as shown below. From the data collected, a plot of the concentration against time was constructed (Figure 14). From this plot, the initial rates of the reactions were calculated and from which the order of the reaction with respect to  $[\text{VO}(\text{O}_2)\text{HEDTA}]^{-2}$  was determined to be first order; Table 3 and Figure 15.

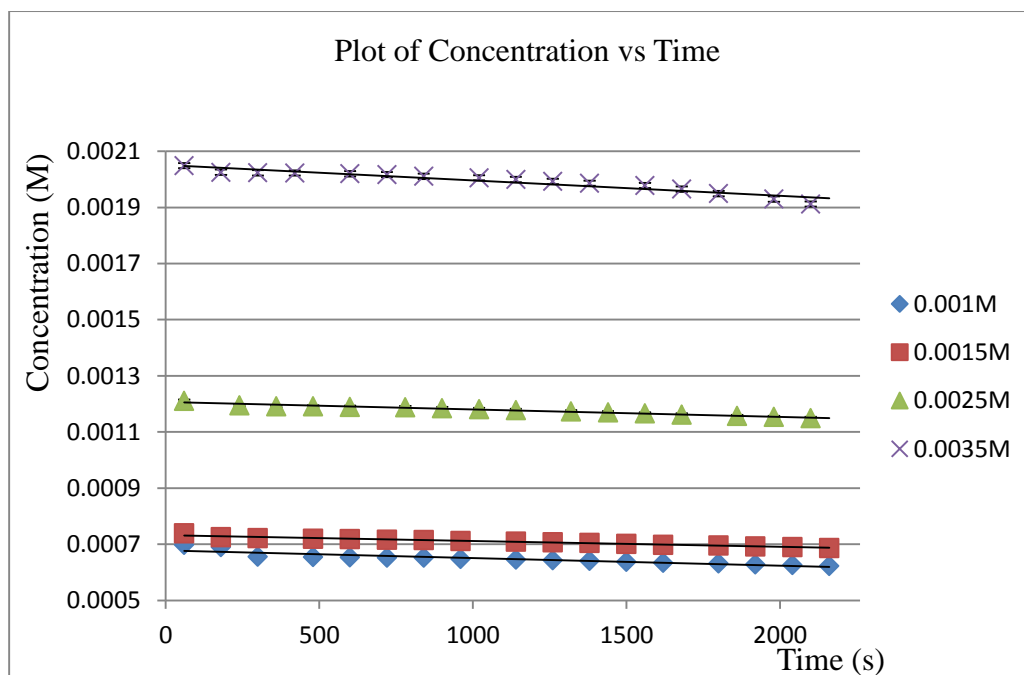


**Figure 14:** Plot of concentration of  $[\text{VO}(\text{O}_2)\text{HEDTA}]^{-2}$  against time.  $[\text{H}^+] = 0.50 \text{ M}$

$$\text{Rate}_i = k\{[\text{VO}(\text{O}_2)\text{HEDTA}]^{-2}\}^n[\text{H}^+]$$

It had been proven that the reaction is first order with respect to the acid concentration. It is assumed that the reaction is also first order with respect to the concentration of  $[\text{VO}(\text{O}_2)\text{HEDTA}]^{-2}$ . A plot of the initial rate against the concentration of  $[\text{VO}(\text{O}_2)\text{HEDTA}]^{-2}$  gave a straight line, which confirms the fact that the reaction is also first order with respect to  $[\text{VO}(\text{O}_2)\text{HEDTA}]^{-2}$ , as shown by a higher  $R^2$  value (0.9368) for first order than for zero (# N/A), half (0.8971) or second (0.2735) orders.

**Table 3:** The Initial Rates and Concentrations for the Various  $[\text{VO}(\text{O}_2)\text{HEDTA}]^{-2}$  Concentrations

| Volume  | Initial rate <sub>i</sub><br>(M/s) | $[\text{VO}(\text{O}_2)\text{HEDTA}]^{-2}$ | $[\text{H}^+]_{\text{calc}}$ | $R^2$  |
|---------|------------------------------------|--|------------------------------|--------|
| 1.00 mL | $1.59 \times 10^{-8}$              | $2.136 \times 10^{-3}$                     | 0.500 M                      | 0.8153 |
| 1.50 mL | $2.21 \times 10^{-8}$              | $3.204 \times 10^{-3}$                     | 0.500 M                      | 0.9647 |
| 2.50 mL | $2.77 \times 10^{-8}$              | $5.340 \times 10^{-3}$                     | 0.500 M                      | 0.9696 |
| 3.50 mL | $4.80 \times 10^{-8}$              | $7.476 \times 10^{-3}$                     | 0.500 M                      | 0.9122 |

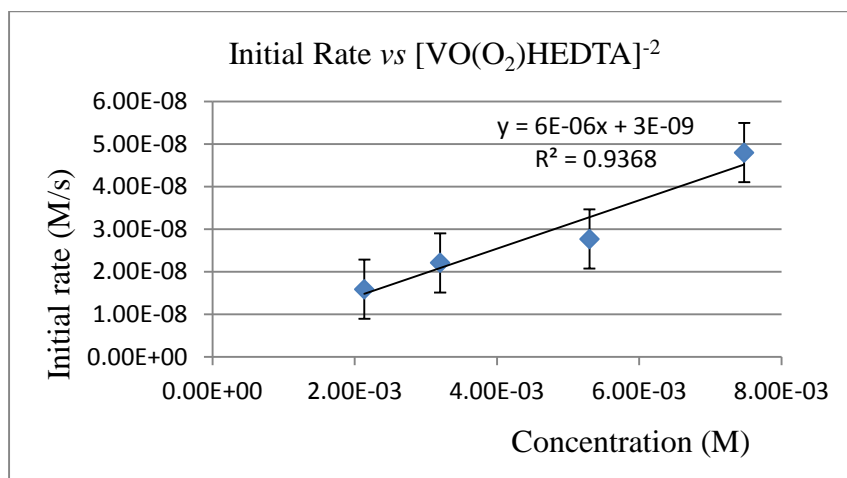


**Figure 15:** A plot of initial rate against concentration of  $[\text{VO}(\text{O}_2)\text{HEDTA}]^{-2}$

From the plot in Figure 15, above, it is seen that the plot gives a straight line. From this it was concluded that the reaction is first order with respect to  $[\text{VO}(\text{O}_2)\text{HEDTA}]^{-2}$  concentration.

Calculations for the rate constant of the reaction are given below.

$$\text{Rate}_i = k_{\text{obs}} [\text{VO}(\text{O}_2)\text{HEDTA}]^{-2}$$

Where  $k_{\text{obs}} = k[\text{H}^+] = 5.696 \times 10^{-6}$ ,  $k = k_{\text{obs}} / [\text{H}^+]$ ,  $[\text{H}^+] = 0.500 \text{ M}$

$$k = 5.696 \times 10^{-6} / 0.500 \text{ M} = 1.14 \times 10^{-5} \pm 1.05 \times 10^{-6} \text{ sM}^{-1} \quad R^2 = 0.9368$$

Calculating The Rate Constant While Changing the Concentration of Acid and  $[\text{VO}(\text{O}_2)\text{HEDTA}]^{-2}$

## <sup>2</sup> Solutions

The rate constant was calculated by reactions of aliquots of 5 mL 1.0 M  $\text{HClO}_4$  (5.0 mmol) with 1 mL (0.02 mmol), 2 mL (0.04 mmol), 3 mL (0.06 mmol), and 4 mL (0.08 mmol) of  $[\text{VO}(\text{O}_2)\text{HEDTA}]^{-2}$  solution. In this experiment, the volume of the reaction mixture was not kept constant such that the concentration of the acid and the  $[\text{VO}(\text{O}_2)\text{HEDTA}]^{-2}$  in solution were changing in the different volume mixtures of the acid and  $[\text{VO}(\text{O}_2)\text{HEDTA}]^{-2}$  solution of the reactions. The plot of the concentration against time was as shown on Figure 16 below, and the data are shown in Table 4 and Figure 17.



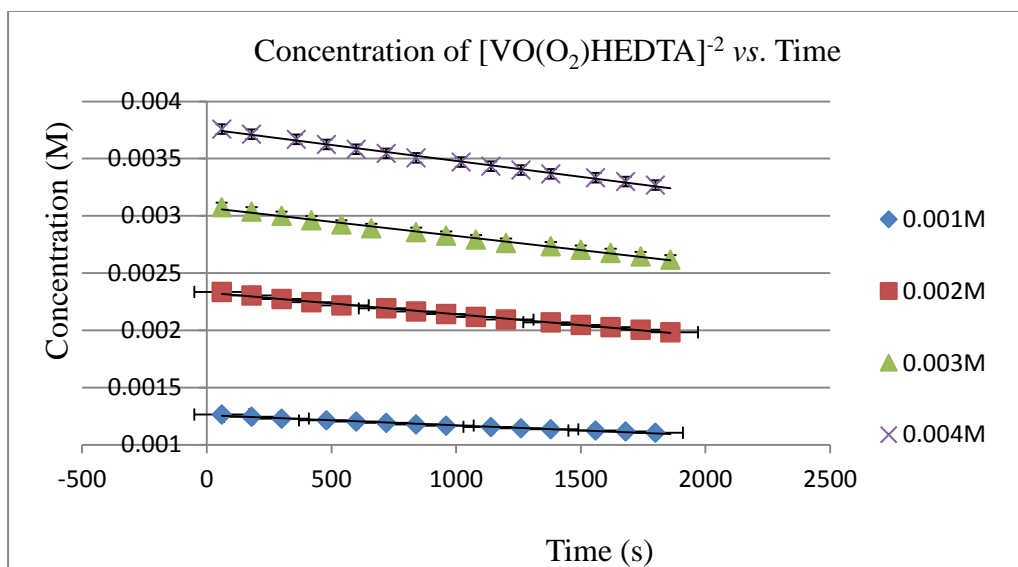


**Figure 16:** Plot of concentration of  $[\text{VO}(\text{O}_2)\text{HEDTA}]^{-2}$  against time

**Table 4:** The Initial Rates and Concentrations for the Various Volumes of Solution

| Volume (mL) | $[\text{VO}(\text{O}_2)]$ M | $[\text{H}^+]$ M | Initial rate (mol/L.s) | k /sM                 | $R^2$  |
|-------------|-----------------------------|------------------|------------------------|-----------------------|--------|
| 1           | $3.30 \times 10^{-3}$       | 0.833            | $9.00 \times 10^{-8}$  | $2.27 \times 10^{-5}$ | 0.9899 |
| 2           | $5.66 \times 10^{-3}$       | 0.714            | $2.00 \times 10^{-7}$  | $2.52 \times 10^{-5}$ | 0.9957 |
| 3           | $7.43 \times 10^{-3}$       | 0.625            | $2.00 \times 10^{-7}$  | $1.68 \times 10^{-5}$ | 0.9952 |
| 4           | $8.80 \times 10^{-3}$       | 0.555            | $3.00 \times 10^{-7}$  | $1.89 \times 10^{-5}$ | 0.9954 |

avg. k =  $2.09 \times 10^{-5} (\text{sM})^{-1}$       std. dev. =  $3.76 \times 10^{-6}$        $R^2 = 0.9941$

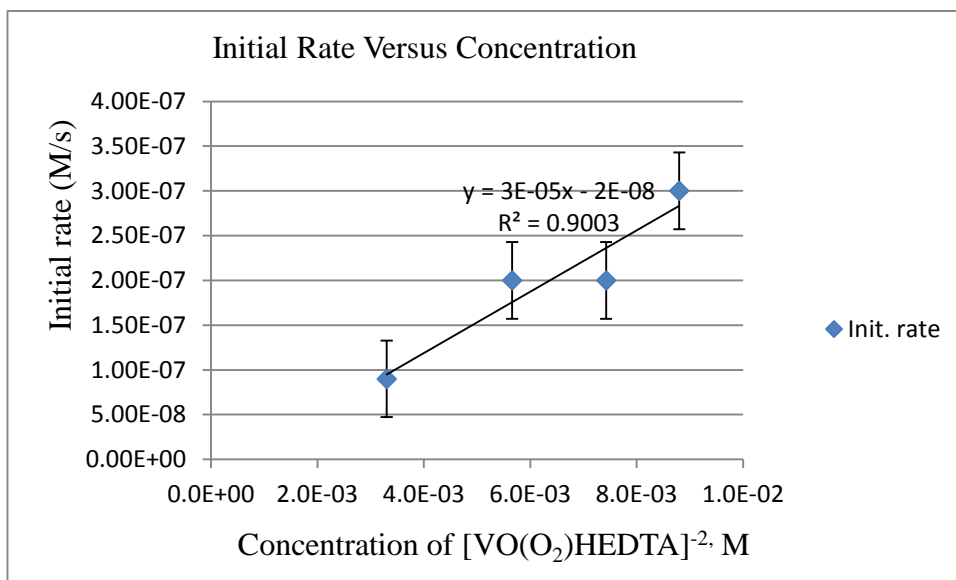


**Figure 17:** A plot of initial rate versus concentration of  $[\text{VO}(\text{O}_2)\text{HEDTA}]^{-2}$

There are three values of the rate constant ( $k$ );  $2.15 \times 10^{-5}$ ,  $2.09 \times 10^{-5}$ ,  $1.14 \times 10^{-5}$ . The average  $k$  value is  $1.79 \times 10^{-5}$  and  $\text{STDV} = 5.666 \times 10^{-6}$ .

$$\Rightarrow k = 1.79 \times 10^{-5} \pm 5.666 \times 10^{-6} (\text{sM})^{-1}$$

The rate equation for the decomposition of  $[\text{VO}(\text{O}_2)\text{HEDTA}]^{-2}$  in the presence of acid is given as;

$$\text{Rate} = 1.79 \times 10^{-5} \{[\text{VO}(\text{O}_2)\text{HEDTA}]^{-2}\}[\text{H}^+] \quad @ 25 \text{ } ^\circ\text{C} \quad (6)$$

The solutions of the reaction mixture, observed after five days of the reaction, showed that the color of the mixture changed over time from the reddish-brown color which represents the vanadium(V) complex to green, and finally to blue. This indicates that the reaction reverses back to the original product of vanadium(IV),  $\text{VO}^{+2}$ .<sup>24</sup> After five days of the reaction, the UV-Visible spectrum of the reaction was taken and is presented in Figure 18.

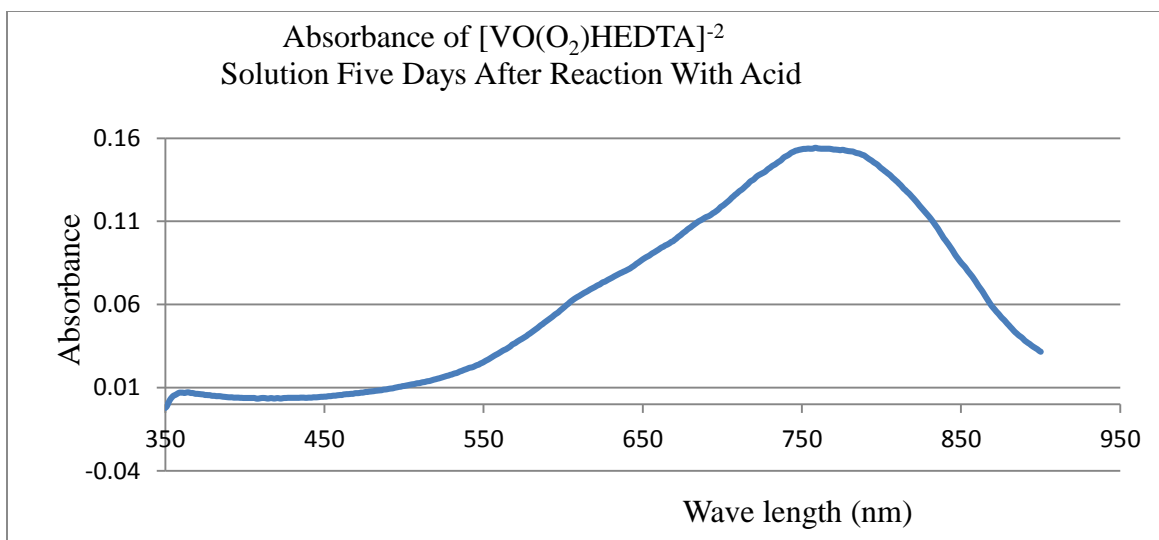


**Figure 18:** UV-Visible spectrum of  $[\text{VO}(\text{O}_2)\text{HEDTA}]^{-2}$  solution five days after reacting with acid

The spectrum is clearly that of a vanadium(IV) solution without any ligand coordinating to the metal oxide. The implication of this is that the decomposition reaction is not limited to the peroxide but involves the de-coordination of the ligand and also the reduction of the metal from the V to the IV oxidation state.

#### Studies on the Catalytic Properties of $[\text{VO}(\text{O}_2)\text{H}_2\text{EDTA}]$

The synthesis gave a fine, bright yellow precipitate of the  $[\text{VO}(\text{O}_2)\text{H}_2\text{EDTA}]$  complex. This complex was analyzed by FT-IR and the spectra are presented below. An analysis of the spectrum of  $\text{H}_3\text{EDTA}$  was made to highlight some of the features of the compound (see Figures 19 and 20). From the spectrum (see Figure 20), the methylene group between two nitrogen's absorbed at  $1445\text{ cm}^{-1}$ , the tertiary amine group absorbed at  $2743\text{ cm}^{-1}$ , the carboxylic group absorbed at  $1626$ , and  $3296\text{ cm}^{-1}$ , and the  $-(\text{CH}_2)$  group absorbed at  $740\text{ cm}^{-1}$  and the hydroxyl group absorbed at  $1081\text{ cm}^{-1}$ .<sup>26</sup>

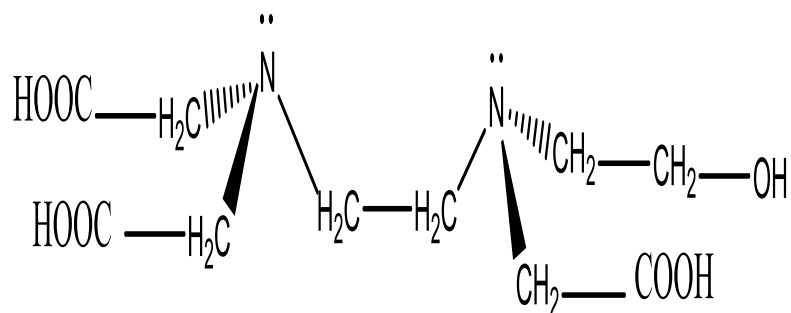


**Figure 19:** Structure of H<sub>3</sub>EDTA

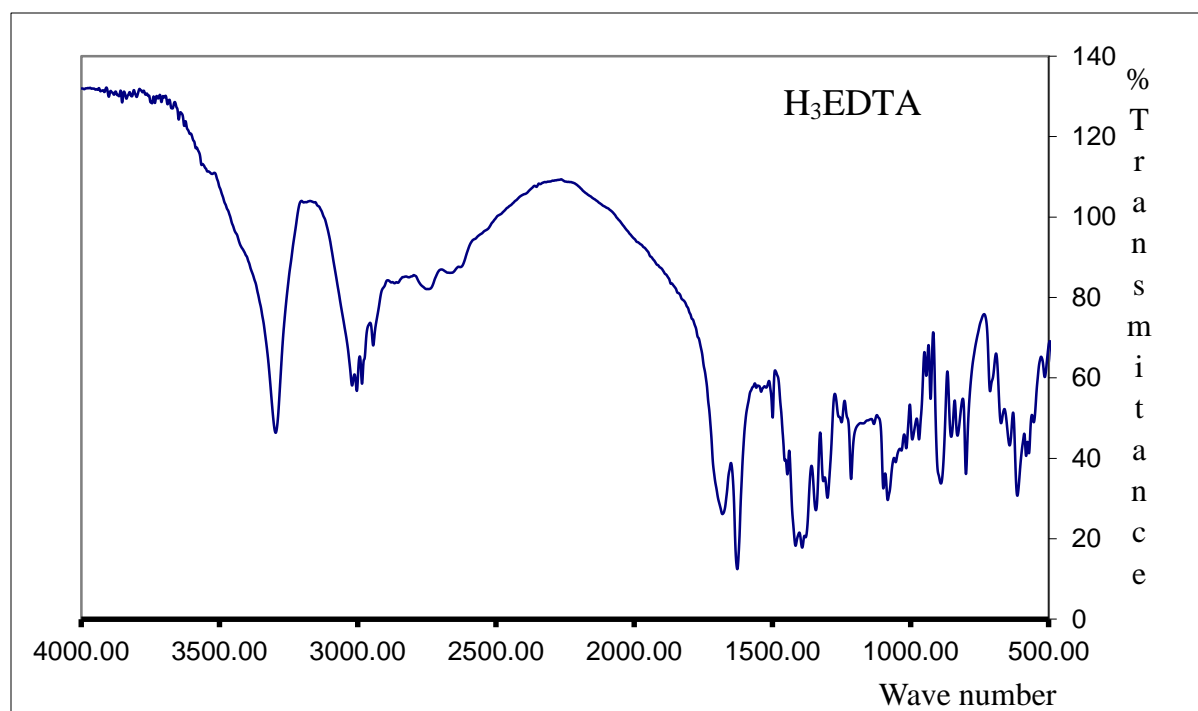


**Figure 20:** FT-IR spectrum of H<sub>3</sub>EDTA

Chelation of H<sub>3</sub>EDTA with the VO(O<sub>2</sub>)<sup>+1</sup> moiety showed an absorbance at 3422 cm<sup>-1</sup>, absorption by carboxylic COOH group at 3235 cm<sup>-1</sup> and 2946 cm<sup>-1</sup>, the tertiary amine showed absorbance at 2611 cm<sup>-1</sup>, deprotonated carboxylic group showed absorbance between 1616-1670 cm<sup>-1</sup>. The methylene groups between two nitrogen's shows an absorbance at 1465 cm<sup>-1</sup>. The V=O group absorbance is observed at 970 cm<sup>-1</sup>. The peroxy O-O group shows absorbance at 938

$\text{cm}^{-1}$  (or  $879 \text{ cm}^{-1}$ ). The V-O group shows absorbance at  $518 \text{ cm}^{-1}$ . The  $-(\text{CH}_2)_2$  group shows absorbance at  $755 \text{ cm}^{-1}$ . All of these observed peaks are characteristic peaks for the vanadium(V) complex and also features of the ligand, which confirms the fact that the yellow precipitate was in effect a complex between vanadium(V) and the  $\text{H}_3\text{EDTA}$  ligand ( see Figure 21).<sup>7,12,10,26</sup>

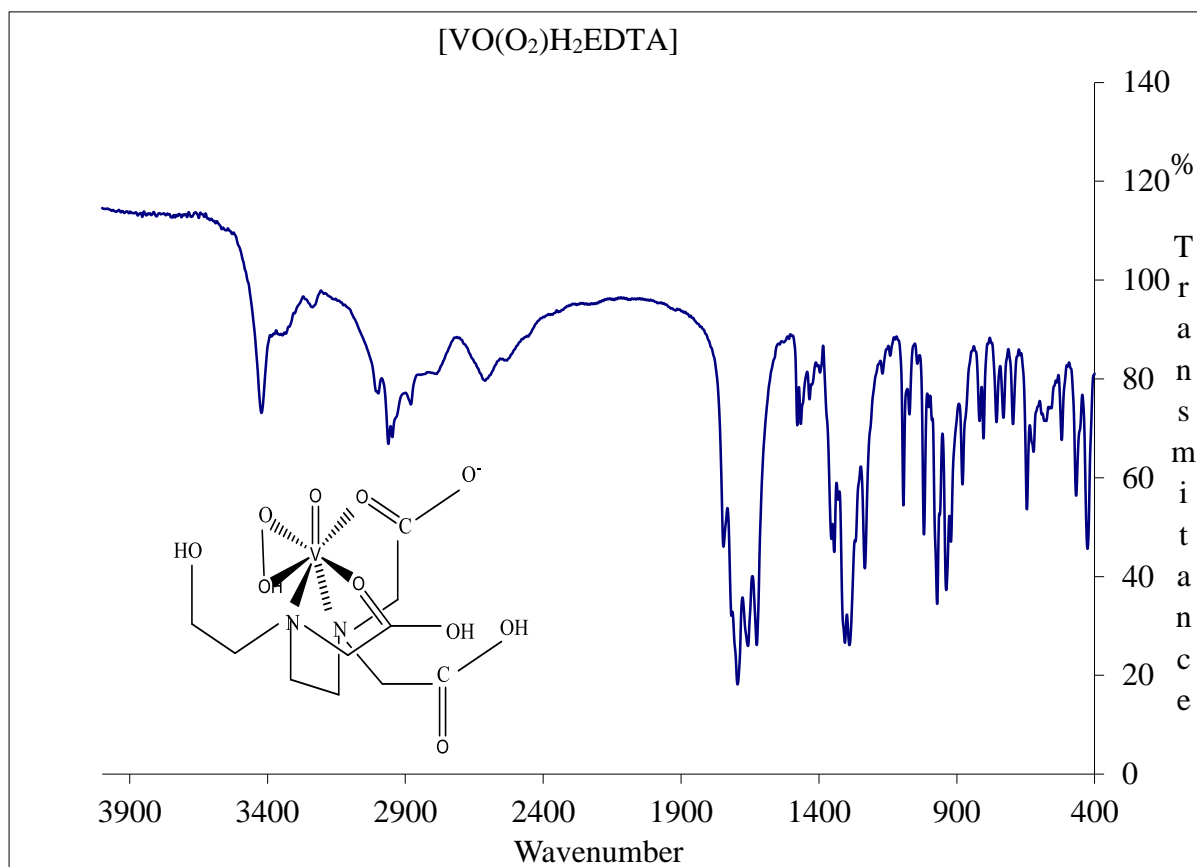


**Figure 21:** FT-IR spectrum of  $[\text{VO}(\text{O}_2)\text{H}_2\text{EDTA}]$

The UV-Vis spectrum in Figure 22 is that of  $[\text{VO}(\text{O}_2)\text{H}_2\text{EDTA}]$  in dimethylsulfoxide. It shows two characteristic absorbance peaks as expected for a vanadium oxoperoxo compound. The intense peak at about 260 nm indicates the presence of the V=O group. The band that starts

at 475 nm and has a peak at about 360 nm represents the absorbance of the vanadium peroxy group. This band is attributed to the vanadium ligand to metal charge transfer (LMCT).<sup>15</sup> It is supposed to have a maximum at about 425 nm but the highly intense peak at 260 nm nearby pulls and stretches the band further towards the more intense peak at 280 nm. The spectrum showed no features beyond 475 nm. From this spectrum it is concluded that the yellow precipitate was a compound of a vanadium(V) oxoperoxy complex.<sup>7,16,10</sup>

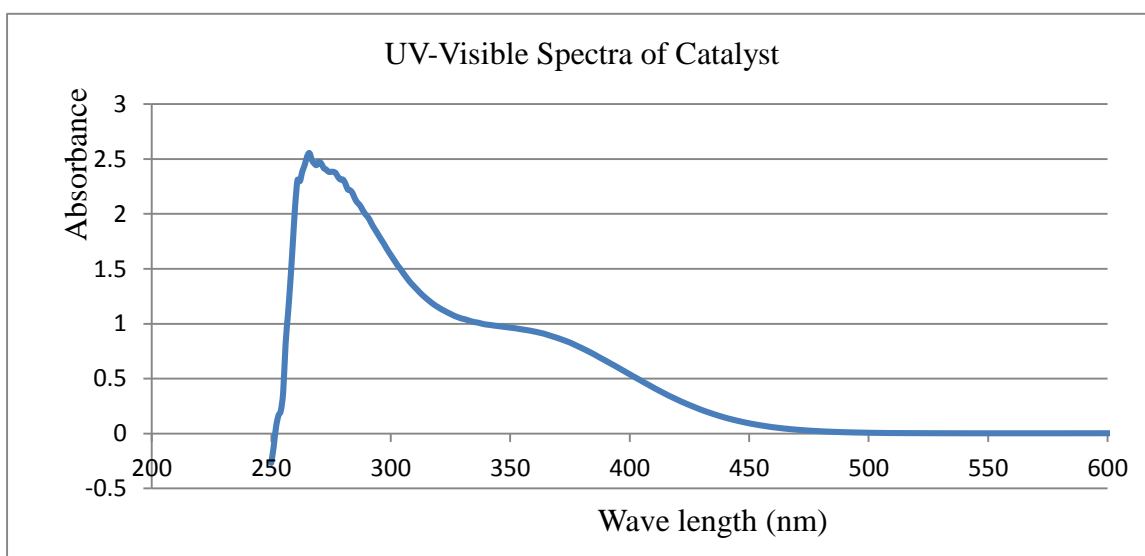


**Figure 22:** The UV-Visible spectrum of  $[\text{VO}(\text{O}_2)\text{H}_2\text{EDTA}]$  in DMSO (CAUTION: can be absorbed through skin)

The yellow product of the synthesis was sent to Galbraith Laboratory for elemental analysis and the results are presented in Table 5 alongside the calculated percentage composition.

The results of the elemental analysis along with the UV-Vis and FT-IR spectroscopy confirmed the fact that the yellow precipitate was a vanadium oxoperoxy complex coordinated to  $\text{H}_3\text{EDTA}$  with formula  $\text{VO}(\text{O}_2)\text{C}_{10}\text{H}_{17}\text{N}_2\text{O}_7$ .

**Table 5:** Results for the Elemental Analysis for [VO(O<sub>2</sub>)H<sub>2</sub>EDTA]

|              | %C    | %H   | %N   | %V    | %O    |
|--------------|-------|------|------|-------|-------|
| Experimental | 34.93 | 4.41 | 7.71 | 13.3  | 39.65 |
| Calculated   | 31.93 | 4.56 | 7.45 | 13.54 | 42.52 |

The catalytic properties of the complex were tested by reacting it with salicylaldehyde in an oxibromination reaction. The products are analyzed by GC-MS and the spectra for the reactions with and without the catalyst are analyzed below, see Figures 23 and 24.

The spectra for the two reactions were identical showing four peaks at almost the same times which indicates the presence of the same products. The peak at about 6.665 min has a mass to charge ratio (m/z) of 122 which is the unreacted C<sub>7</sub>O<sub>2</sub>H<sub>6</sub> with molecular mass 122, as seen on Figure 25 below.

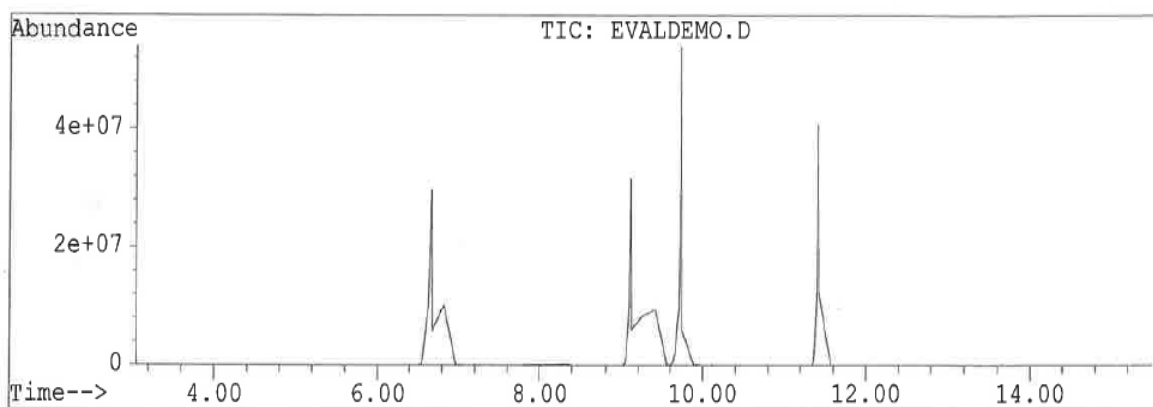


**Figure 23:** The GC-MS of the oxibromination reaction of salicylaldehyde without the catalyst

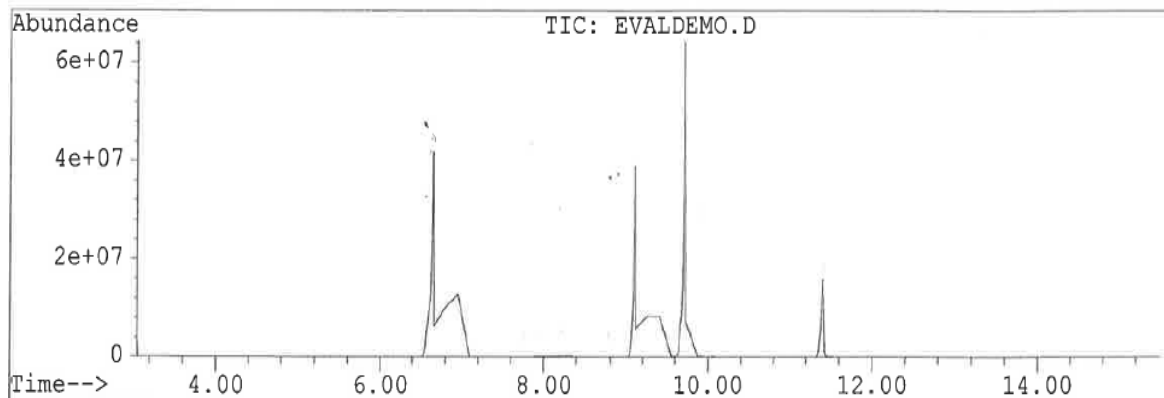


**Figure 24:** The GC-MS of the oxibromination reaction of salicylaldehyde with  $\text{VO}(\text{O}_2)\text{C}_{10}\text{H}_{17}\text{N}_2\text{O}_7$ , ([ $\text{VO}(\text{O}_2)\text{H}_2\text{EDTA}$ ])

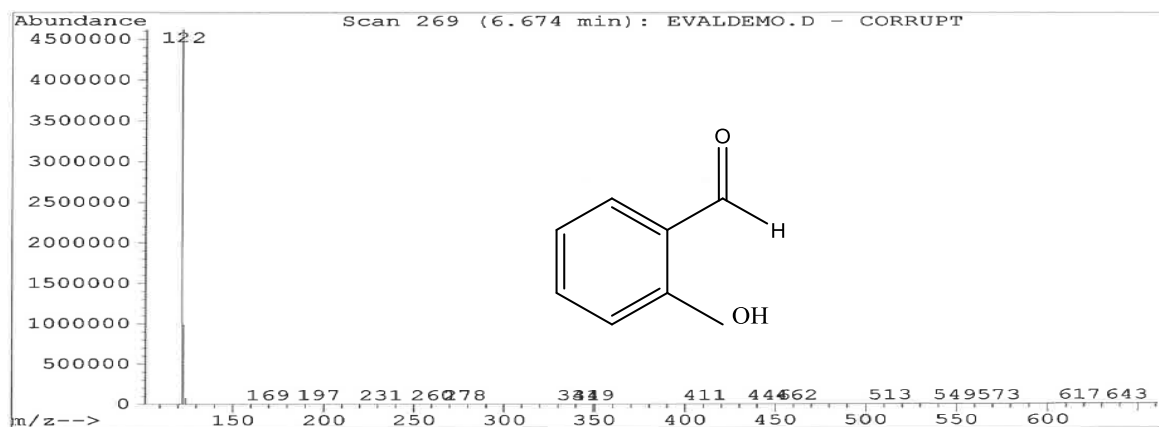
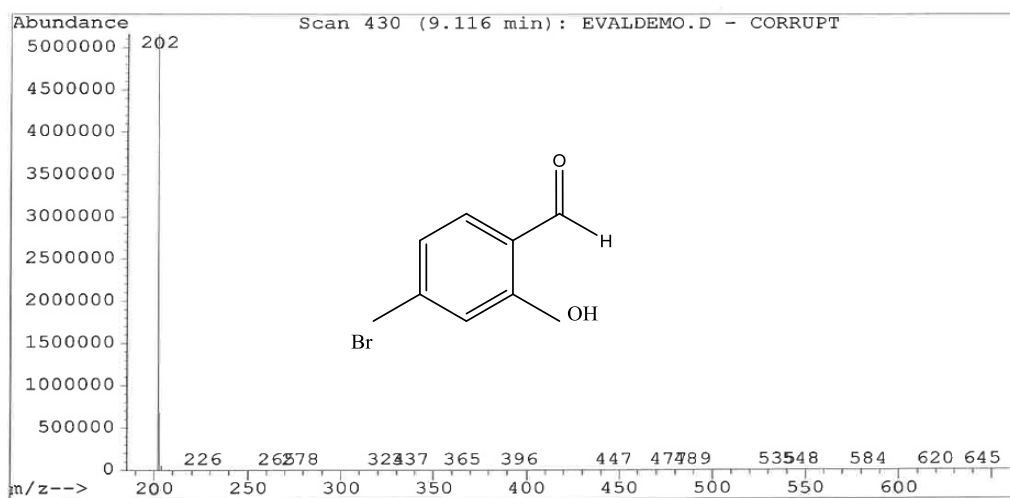


**Figure 25:** MS spectrum for peak at 6.674 min which is  $\text{HOC}_6\text{H}_4\text{CHO}$  and structure

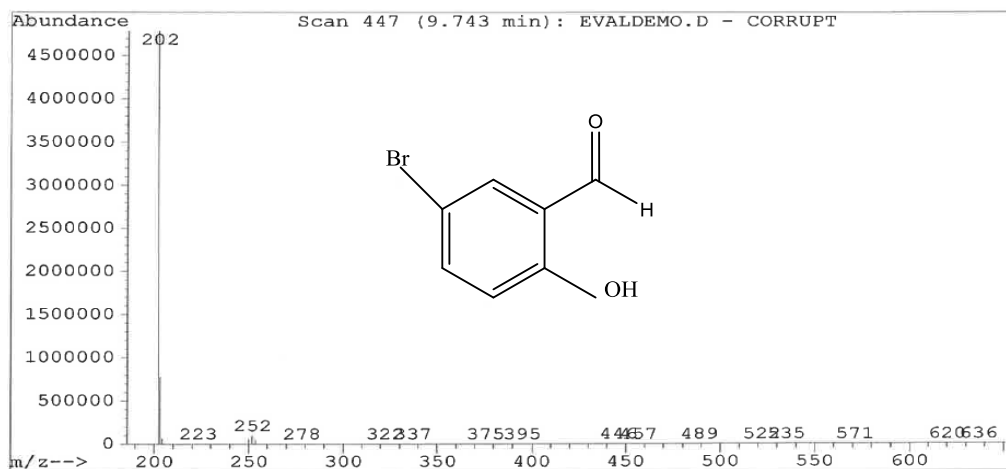
The peak at 9.116 min and 9.743 min for the reaction without catalyst is for the monobrominated product (see Figure 26 and 27) that indicates a possible isomer with molecular formula  $\text{HOC}_6\text{H}_3\text{CHOBr}$  and molecular mass of 202. The peak at 9.118 min for the reaction with a catalyst has an m/z of 202 that is the monobrominated product of the salicylaldehyde with the same formula and mass as above, see Figure 28. Bromine has two isotopes,  $^{79}\text{Br}$  and  $^{81}\text{Br}$ , with relative abundance of 50.69 % and 49.31 %, respectively. This gives rise to peaks with relative intensity ratios 1:1 for a monobromination, 1:2:1 for a dibromination, and 1:3:3:1 for a



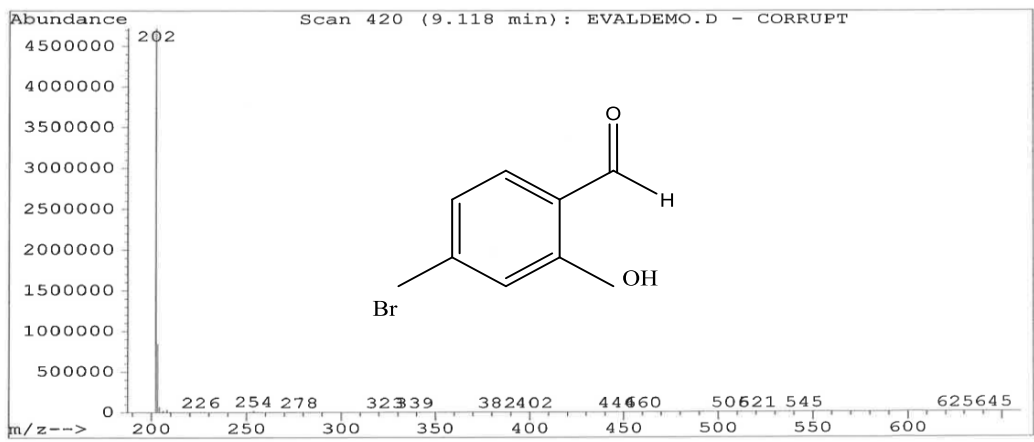
tribrominated product.<sup>25</sup> In the reaction without the catalyst, there are two peaks for the monobrominated product, one at 9.743 min., and one at 9.116 min as observed in Figures 26 and 27 below. Both reaction conditions have peaks at 11.40 min which had a m/z of 280. This peak has three peaks with intensity an ratio in the ratio 1:2:1 indicating the dibrominated product (Figure 29 and 30).<sup>25</sup>



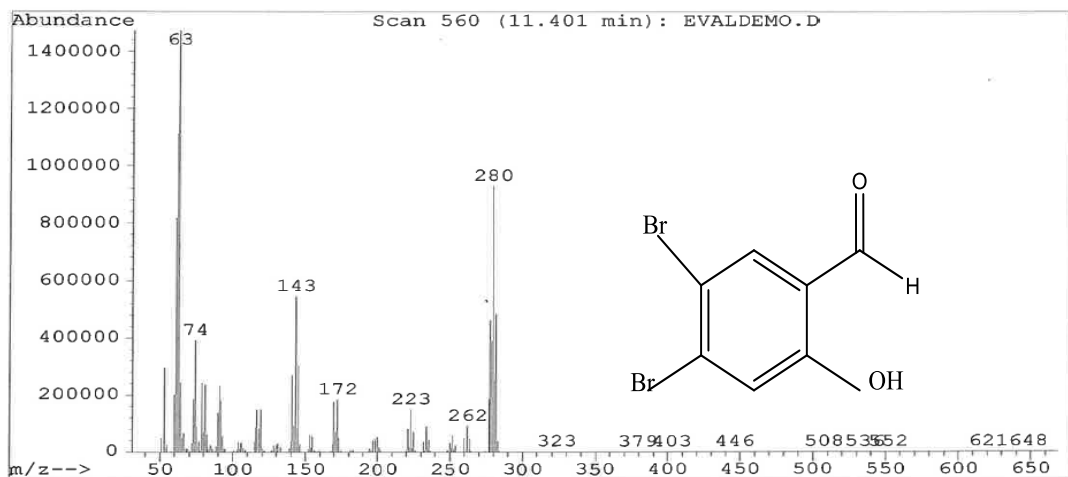
**Figure 26:** MS spectrum for peak at 9.116 min for reaction without catalyst



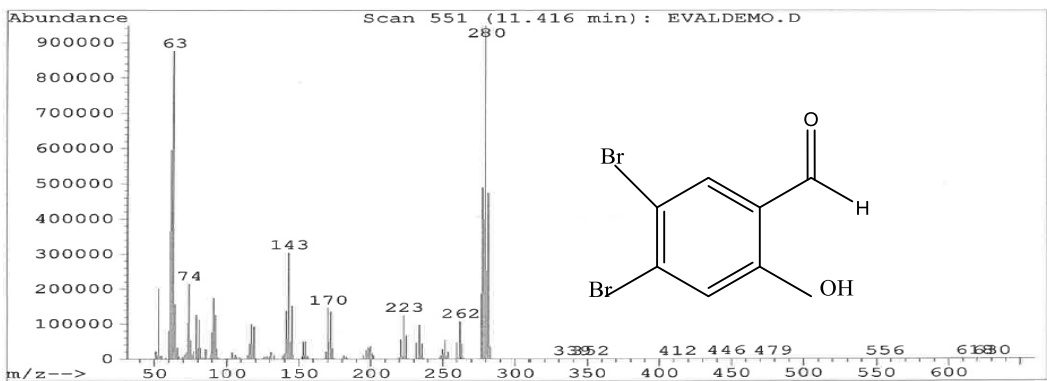
**Figure 27:** The MS spectrum for peak at 9.743 min for reaction without catalyst



**Figure 28:** The MS spectrum for peak at 9.118 min for reaction with catalyst

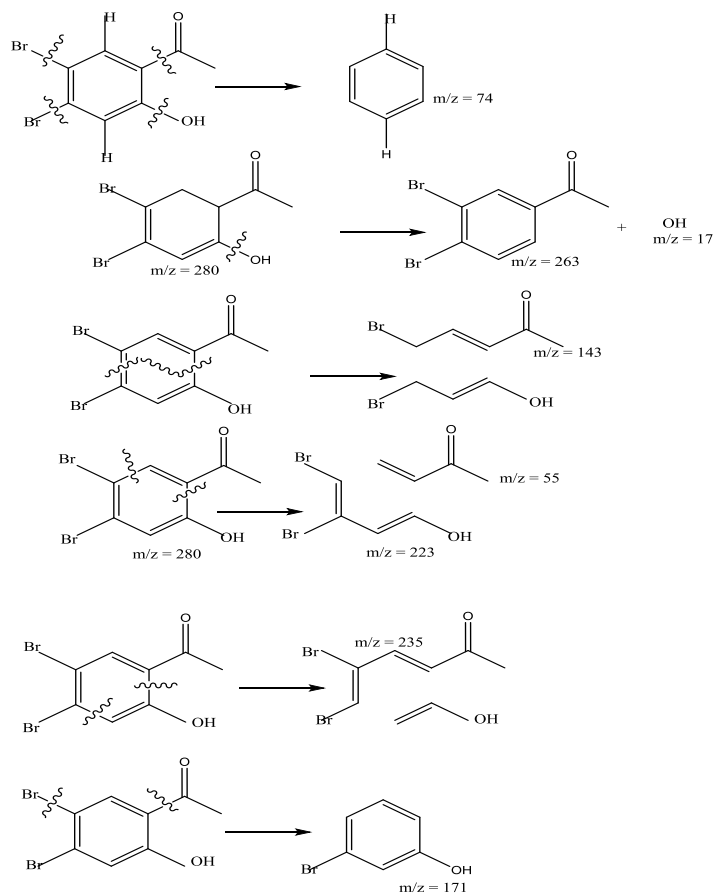


**Figure 29:** The spectrum for the peak at 11.401 min for the reaction without catalyst



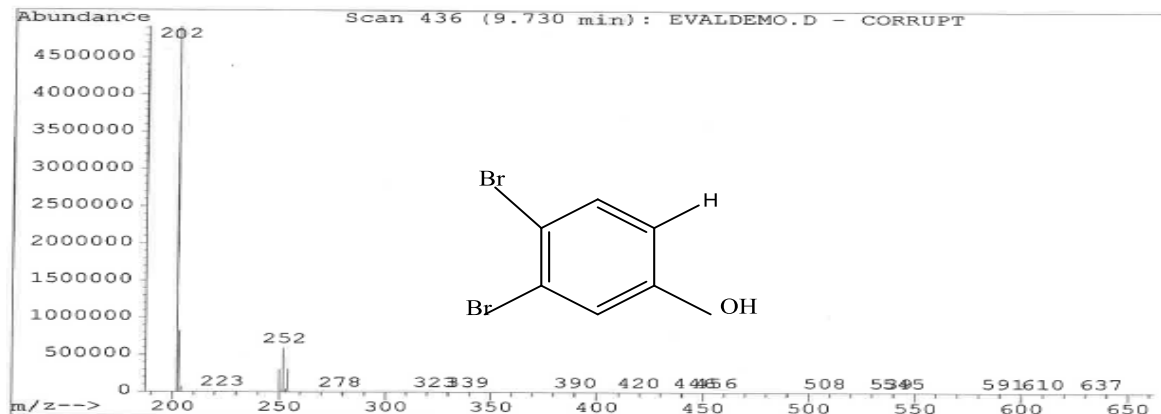
**Figure 30:** The MS spectrum for the peak at 11.416 min for the reaction with catalyst

Figure 31, below, represents the fragmentation that accounts for the peaks on the spectra. The wavy lines cut across the bonds that are broken in the fragmentation process.



**Figure 31:** Fragmentation patterns for peaks with  $m/z$  280

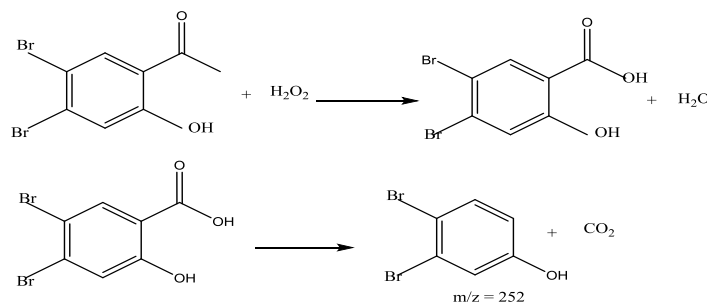
The reaction with the catalyst gives a peak at 9.730 min with an  $m/z$  ratio of 252 as can be seen in Figure 32 below.



**Figure 32:** The GC-MS for the reaction with a catalyst for the peak at 9.730 min with an m/z of

252

The peak at 9.730 min with an m/z ratio of 252 corresponds to a dibromination with decarboxylation which removes the C=O group, (Figure 32).



This peak has three peaks with a relative intensity ratio of 1:2:1, which were the identifying peak for a dibrominated product.<sup>25</sup> The reaction was done without acid both with and without a catalyst and the results in the absence of an acid showed no difference from the reactions where there was an acid.

Tables 6 and 7 summarize the product distribution in the catalyzed and uncatalyzed arylbrominations.

From Tables 6 and 7 below, it can be concluded that the extent of conversion is greater for the reaction without the catalyst than for the reaction with a catalyst. The relative abundance of the unreacted salicylaldehyde is  $4.0 \times 10^7$  for the reaction with catalyst, while it is  $3.0 \times 10^7$  for the reaction without the catalyst, indicating there was more conversion in the reaction without catalyst than that with catalyst. The reaction with the catalyst gave three distinct products, while that without the catalyst gave two. The article from which the reaction was copied did not report any control reaction, and the catalyst was polymer-grafted.<sup>22</sup> The reaction does not need a catalyst because the control reaction gives the same products as that with the catalyst. The only observable effect of the catalyst is in the distribution of the products.

**Table 6:** Summary of Results from GC-MS Analysis of Reaction without a Catalyst

| M/Z ratio | Time (min) | Abundance         |
|-----------|------------|-------------------|
| 122       | 6.678      | $3.0 \times 10^7$ |
| 202       | 9.116      | $3.2 \times 10^7$ |
| 202       | 9.743      | $5.2 \times 10^7$ |
| 280       | 11.401     | $4.0 \times 10^7$ |

**Table 7:** Summary of Results from GC-MS Analysis of Reaction with Catalyst

| M/Z ratio | Time (min) | Abundance         |
|-----------|------------|-------------------|
| 122       | 6.663      | $4.0 \times 10^7$ |
| 202       | 9.118      | $3.6 \times 10^7$ |
| 252       | 9.730      | $6.4 \times 10^7$ |
| 280       | 11.416     | $1.6 \times 10^7$ |

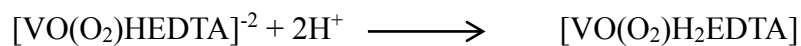
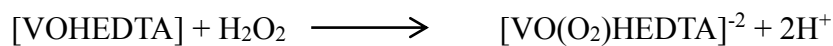
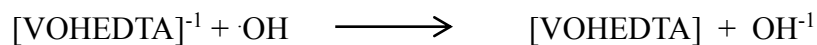
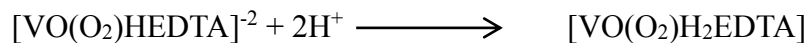
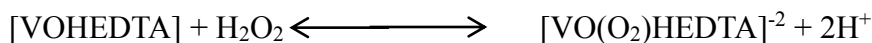
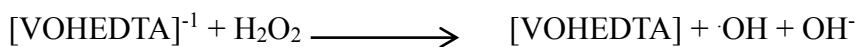
## CHAPTER 4

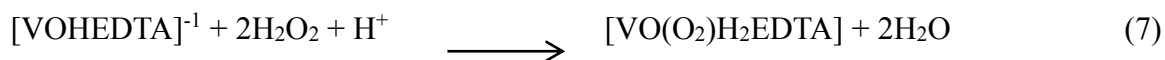
### DISCUSSION

The UV-Visible spectrum of a 0.100M solution of  $\text{VO}(\text{ClO}_4)_2$  gives a peak at 760 nm ( $\epsilon = 15.9 \text{ cm}^{-1}\text{M}^{-1}$ ) a characteristic peak of  $\text{VO}^{2+}$  compounds that confirms the fact that the solution is that of  $\text{VO}(\text{ClO}_4)_2$ . The molar extinction coefficient is within the range expected for the solution.<sup>28</sup> The solution of  $[\text{VO}(\text{HEDTA})]^{-1}$  gives two peaks; one at 580 nm and one at 775 nm ( $\epsilon = 21.5 \text{ cm}^{-1}\text{M}^{-1}$ ). These peaks confirm the complexation of  $\text{H}_3\text{EDTA}$  onto the  $\text{VO}^{2+}$  group. As  $\text{H}_2\text{O}_2$  is added to the  $[\text{VO}(\text{HEDTA})]^{-1}$  solution, there is a gradual decay of the peak at 775 nm and an increase for the peak at 425 nm. The peak at 580 nm exhibits an isobestic point. The peak at 425 nm is characteristic of the  $\text{VO}(\text{O}_2)^+$  moiety. This peak confirms the presence of vanadium(V) oxoperoxo compound. The decrease in the peak at 775 nm indicates the oxidation of the vanadium(IV) to a vanadium(V) complex. The isobestic point indicates a smooth transition from the reactant to the product without any intermediate. At the end of the reaction, the solution gives a peak at 425 nm with a molar extinction coefficient of  $227.78 \text{ cm}^{-1}\text{M}^{-1}$ , which is within the range for the  $\text{VO}(\text{O}_2)^+$  group. This confirms the fact that the solution is a product of the vanadium(V) oxoperoxo moiety.<sup>22</sup>

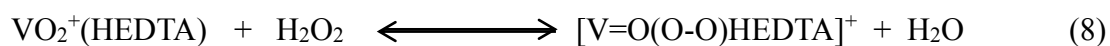
The studies of the effects of acid concentration on the rate of the reaction between  $\text{H}_2\text{O}_2$  and  $[\text{VOHEDTA}]^{-1}$  solution give consistent results. In the first part of the study, as the  $[\text{H}^+]$  is varied, the absorbance at 425 nm decreases as a result of the decomposition of

$[\text{VO}(\text{O}_2)\text{HEDTA}]^{-2}$ . A plot of the change in absorbance against time gives straight lines for the various trials. The slopes of the line were plotted against the concentration and give straight lines that indicates the decomposition reaction is first order with respect to  $[\text{H}^+]$ . When the  $[\text{H}^+]$  concentration was kept constant and the  $[\text{VO}(\text{O}_2)\text{HEDTA}]^{-2}$  solution was varied, the plot of initial rates against time gave a straight line that confirmed the fact that the reaction is also first order with respect to the concentration of  $[\text{VO}(\text{O}_2)\text{HEDTA}]^{-2}$ . It was also observed that as the acid reacted with the  $[\text{VO}(\text{O}_2)\text{HEDTA}]^{-2}$  in solution, the peak at 425 nm decreased in absorbance but the peak at 775 nm did not indicate a simultaneous increase in absorbance. Because protonation reactions are typically fast, a direct reaction between  $[\text{VO}(\text{O}_2)\text{HEDTA}]^{-1}$  and  $[\text{H}^+]$  is the initiation step.



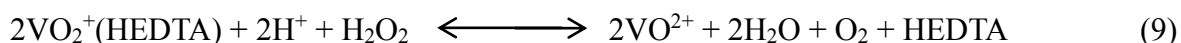


Suggestions were made that the decomposition reaction of  $[\text{VO}(\text{O}_2)\text{HEDTA}]^{-2}$  in acid solution appears to take place in two stages; initially, a rapid equilibrium is established.<sup>27</sup>



The equilibrium for the reaction lies far to right, which favours the  $[\text{OV}(\text{O}-\text{O})]^+$  complex.<sup>27</sup>

When acid was added, it displaced the equilibrium to the left by reaction with the  $\text{VO}_2^+$  species.



This shifted the equilibrium to the left and gradually reduced the yellow  $[\text{OV}(\text{O}-\text{O})]^+$  to blue  $\text{VO}^{2+}$ .<sup>27</sup>

Observing the UV-Visible spectrum of the solution of the reaction between  $[\text{VO}(\text{O}_2)\text{HEDTA}]^{-2}$  and acid after five days of the reaction, the spectrum shows only one band at 775 nm without any complexation, which indicates the presence of  $\text{VO}^{2+}$  group. This indicates that the decomposition reaction is a decomplexation of the  $\text{H}_3\text{EDTA}$  and a reduction from the vanadium(V) to the vanadium(IV) oxidation state.

The synthesis of a solid catalyst ( $^{\text{n}4}$ -[N-(2-hydroxyethyl)ethylenediamine-N,N,N-triacetic acid]-oxo- $^{\text{n}2}$ -peroxovanadium(V) complex) gave a bright yellow precipitate. Elemental analysis established its formula as  $[\text{VO}(\text{O}_2)\text{H}_2\text{EDTA}]$ . According to the literature, the color of such a



complex should be between yellow and orange.<sup>22</sup> The FT-IR spectrum shows vibrations for all the characteristic peaks of the  $\text{VO}(\text{O}_2)^+$  moiety, the  $\text{H}_3\text{EDTA}$  ligand, and also chelation. This confirms the fact that the yellow precipitate is a complex of  $\text{VO}(\text{O}_2)^+$  and  $\text{H}_3\text{EDTA}$  in which the  $\text{H}_3\text{EDTA}$  complexes to the  $\text{VO}(\text{O}_2)^+$  moiety by chelation. The solution of the complex in DMSO shows two peaks; an intense peak and a less intense peak close to each other. The intense peak at 260 nm is characteristic of  $\text{V}=\text{O}$  compounds, while the band that began at 450 nm is seen at 425 nm. This peak is shifted by the very intense peak nearby. The combined data above confirmed the fact that the bright yellow compound was a  $\text{VO}(\text{O}_2)^+$  complex with  $\text{H}_3\text{EDTA}$  with the formula  $[\text{VO}(\text{O}_2)(\text{H}_2\text{EDTA})]$  in which the  $\text{H}_2\text{EDTA}^{-1}$  was a tetradentate ligand. The structure of the complex can be represented as shown in Figure 33 below.

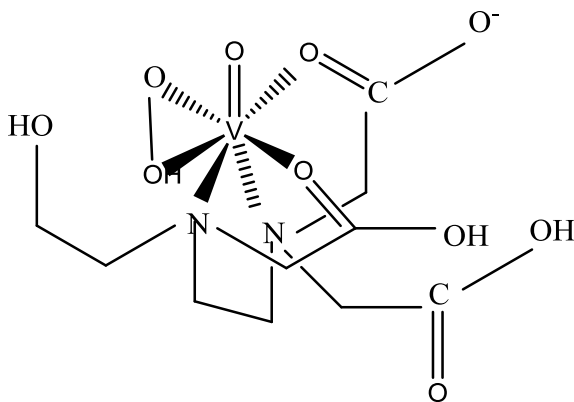


**Figure 33:** The structure of  $[\text{VO}(\text{O}_2)\text{H}_2\text{EDTA}]$

Studies for the catalytic properties of the yellow complex showed that the catalyst favored monooxibromination of salicylaldehyde. The experimental procedure was taken from a published article.<sup>22</sup> The catalyst also forms a dibromoproduct with decarboxylation of the C=O group. The C=O is oxidized to a carboxylic group after which decarboxylation occurred by elimination of CO<sub>2</sub>. The catalyst caused the decarboxylation reaction of the C=O group that is not seen in the control reaction. The catalyst was also tested in the absence of an acid and no difference in the products could be observed by GC-MS. During the course of the experiments investigating the catalytic properties of the yellow precipitate, a control reaction without catalyst was performed. It was observed that the arylbromination reaction occurred even in the absence of the catalyst. A thorough reading of the literature reference showed the lack of any such control reactions. This cast doubts on the reliability of the results in the reference because the arylbromination reaction occurred without the catalyst. The results showed that the presence of the catalyst altered the reaction system in that different ratios of products were obtained.

### Future Work

For the kinetic studies, future work may be done by examining the effects of VO<sup>+2</sup> and H<sub>2</sub>O<sub>2</sub> on the rate of decomposition of [VO(O<sub>2</sub>)HEDTA]<sup>-2</sup> in aqueous media. The catalyst should be tested on other reactions. A crystal should be grown of the catalyst. The crystal will be studied by x-ray crystallography to determine the exact structure of the complex.

## REFERENCES

1. Gorzsas, A. Thesis, Department of Chemistry, Inorganic chemistry, Umea University Sweden, **2005**, 1-8.
2. Srivastava, A. K.; Mehdi, M. Z. Diabetes UK. *Diabetic Medicine*, **2004**, 22, 2-13.
3. Badmaev, V.; Pralash, S.; Majeed, M. *The Journal of Alternative and Complementary Medicine*, **1999**, 5(3), 273-291.
4. Bailar, J. C.; Emelelus, H. J.; Nyholm, R.; Trotman-Dickenson, A. F. *Comprehensive Inorganic Chemistry*, Volume 3, Pergamon Press, **1973**, 491-551.
5. Newton, D. E.; Baker, L. W. *Chemical Elements From Carbon to Krypton*, Vol 3, U. X. L. An imprint of the Gale Group, **1999**, 647-652.
6. Justino, L. L.; Ramos, G. M. L.; Caldeira, M. M.; Gil, V. M. S. *Eur. J. Inorg. Chem.* **2000**, 1617-1621.
7. Waidmann, C. R.; Dipasquale A. G.; Mayer, J. M. *Inorg. Chem.* **2010**, 49, 2383-2391.
8. Mahajan, S.; Singh B.; Sheikh, H. N.; Kalsotra, B. L. *Chemical Science Transactions*, **2012**, 1 (1), 23-34.
9. Bertolini, O.; Conte, V. *J. Inorg. Biochem.*, (**2005**), 99, 1549-1557.
10. Tatiarsky, J.; Pacigova, S.; Sivak, M.; Schwendt, P. *The Journal of the Argentine Chem. Soc.* **2009**, 97(1), 181-198.
11. Kalita, D.; Sarmah, S.; Das, S. P.; Baishya, D.; Patowary, A.; Baruah, S.; Islam, N.S. *Reactive and Functional Polymers*, **2008**, 68, 876-890.
12. Chakravorti, M. C.; Ganguly, S.; Bhattacharjee, M. *Polyhedron*, **1994**, 13(4), 695-699.
13. Chrappova, J.; Schwendt, P.; Dudasova, D.; Tatiarsky, J.; Marek, J. *Polyhedron*, **2008**, 27, 641-647.

14. Schwendt, P.; Dudasova, D.; Chrappova, J.; Drabik, M. ; Marek, J. *J. of Thermal Analysis and Calorimetry*, **2008**, *91*(1), 293-297.
15. Simunekova, M.; Simunek, J.; Chrappova, J.; Schwendt, P. *Inorg. Chem.Commun.* **2012**, *24*, 125-128.
16. Gabriel, C.; Kaliva, M.; Venetis, J.; Baran, P.; Rodriguez-Es-Cudero, I.; Voyiatzis, G.; Zervou, M.; Salifoglou, A. *Inorg. Chem.* **2009**, *48*, 476-487. 16a. Reprinted with permission from Gabriel, C.; Kaliva, M.; Venetis, J.; Baran, P.; Rodriguez-Es-Cudero, I.; Voyiatzis, G.; Zervou, M.; Salifoglou, A. *Inorg. Chem.* **2009**, *48*, 476-487, Copyright 2009 American Chemical Society.
17. Liochev, S. I.; Fridovich, I. *Archives of Biochemistry and Biophysics*, **1991**, *291*(2), 379-382.
18. Zampella, G.; Fantucci, P. ; Pecore, V. L.; L. D. Gioia, *J. Am. Chem. Soc.*,**2005**, *127*, 953-960. 18a. Reprinted with permission from Zampella, G.; Fantucci, P. ; Pecore, V. L.; Gioia, L. D. *J. of American Chem. Soc.*,**2005**, *127*, 953-960, Copyright 2005 American Chemical Society.
19. Patel, H. Department of Chemistry, ETSU, Report Submitted December 15, 2011.
20. Sivak, M.; Mada'rova, M.; Tatiarsky, J.; Marek, J. *Eur. J. Inorg. Chem.* **2003**, 2075-2081. 20a. Reprinted with permission from Sivak, M.; Mada'rova, M.; Tatiarsky, J.; Marek, J. *Eur. J. Inorg. Chem.* **2003**, 2075-2081, Copyright 2003 Elsevier.
21. Campbell, E. C. Presented at the Boland Symposium, East Tennessee State University, March **2014**.
22. Maurya, M. R.; Chaudhary, N. ; Avecilla, F. *Polyhedron*, **2014**, *67*, 436-448. 2014.

23. Singh, R. P.; Kumar, S.; Kumar, P. C.; Chaudhary, R. *Oriental J. O. Chem.*, **2008**, *24*(3), 1057-1062.
24. Ballhausen, C. J. ; Gray, H. B. *Inorg. Chem*, **1962**, *1*, 111-112.
25. McLafferty, F. W. *Interpretation of Mass Spectra*, W. A. Benjamin, Inc. **1966**, pp 16 and 22-26.
26. Speight, J. G. *Lange's Handbook of Chemistry*, Sixteenth Edition, McGraw. Hill, Inc., **2005**, *3*, 6-22
27. Kakabadse, G.; Wilson, H. J. *Chemistry Department The University of Birmingham*, **1960**, *15*, 2475-2479.
28. Alberico, E.; Micera, G.; Sanna, D. *Pergamon*, **1994**, *13* (11), 1763-1771.
29. Atkins, P.; Overton, T.; Rourke, J.; Weller, M.; Armstrong, F. *Shriver & Atkins Inorganic Chemistry*, Fifth Edition, Oxford University Press, **2010**, 474 – 499.

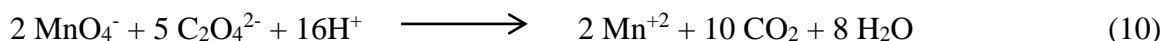
## APPENDIX

### Standardization of KMnO<sub>4</sub> and VO<sup>2+</sup> Solutions

A 0.05 M aqueous solution of KMnO<sub>4</sub> was prepared by dissolving 7.902 g (0.050 mol) of KMnO<sub>4</sub> in 1.00 L of deionized water in a 1.00 L volumetric flask. Two samples of 0.385 g (2.84 x 10<sup>-3</sup> moles) of Na<sub>2</sub>C<sub>2</sub>O<sub>4</sub> were prepared by weighing out and dissolved in 25 mL of deionized water and 10.0 mL of 3.0 M H<sub>2</sub>SO<sub>4</sub> added to samples in a conical flask. The solutions were heated to a temperature of 70 °C. The solutions were titrated with KMnO<sub>4</sub> from a 25 mL burette.

**Table A1:** Titer Values for Standardising Potassium Permanganate

| Sample                  | 1/ mL | 2/ mL |
|-------------------------|-------|-------|
| Initial Burette Reading | 0.00  | 0.00  |
| Final Burette Reading   | 22.10 | 21.90 |
| Titter                  | 22.10 | 21.90 |



Moles of C<sub>2</sub>O<sub>4</sub><sup>2-</sup> in solution = 0.385 g/134 g = 2.873 x 10<sup>-3</sup> moles

Moles of MnO<sub>4</sub><sup>2-</sup> = n(C<sub>2</sub>O<sub>4</sub><sup>2-</sup>) x 2/5 = 2.873 x 10<sup>-3</sup> x 2/5 = 1.149 x 10<sup>-3</sup> moles

Molarity of MnO<sub>4</sub><sup>2-</sup> = 1.149 x 10<sup>-3</sup> moles/ 22.10 x 10<sup>-3</sup> dm<sup>3</sup> OR 1.149 x 10<sup>-3</sup>/ 21.90 x 10<sup>-3</sup> = 5.200 x 10<sup>-2</sup> M or 5.248 x 10<sup>-2</sup> M.

Molarity of KMnO<sub>4</sub> = 0.05248 M

For VO<sup>2+</sup> analyses, 20.00 mL of 0.05248 M KMnO<sub>4</sub> solution was measured into a 100.0 mL volumetric flask and deionized water added to 100.0 mL mark.

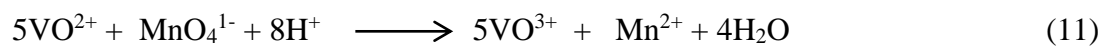
Molarity of new  $\text{KMnO}_4$  solution =  $0.05248 \text{ M} \times 20 \text{ mL}/100.0 \text{ mL} = 0.0104 \text{ M}$

The  $\text{VO}^{2+}$  solution was standardized by pipetting 5.00 mL of the solution in to a conical flask. 10 mL of 3.0 M  $\text{H}_2\text{SO}_4$  was pipetted in to the flask and titrated against 0.0104 M  $\text{KMnO}_4$  from a 25 mL burette. The results of the titration are shown below.

**Table A2:** Titer Values for Standardizing Vanadium(IV) Perchlorate Solution

| Sample                  | 1    | 2     |
|-------------------------|------|-------|
| Initial Burette Reading | 0.00 | 9.85  |
| Final Burette Reading   | 9.85 | 19.55 |
| Titer                   | 9.85 | 9.70  |

Average titer = 9.78



Mole ratio = 5:1

$$[\text{VO}^{2+}] = (5 \times 9.78 \text{ mL} \times 0.0104 \text{ M})/5.0 \text{ mL} = 0.1017 = 0.102 \text{ M} \quad (12)$$

## VITA

### TINGA CLIFORD OYOMBE FON

- Education: B.Sc. Chemistry, University of Buea, Buea Cameroon, 2003
- DIPES II, Higher Teachers Training College University of  
Yaoundé I, Yaoundé, Cameroon, 2006
- Honours Degree in Chemistry, University of the Western Cape,  
Cape Town, South Africa, 2012
- M.Sc. Chemistry, East Tennessee State University, Johnson City,  
Tennessee U.S.A., 2014
- Professional Experience: Mathematics teacher, International School Complex Bastos  
Yaoundé, Yaoundé Cameroon, 2006-2007
- Chemistry /Physics/ Mathematics teacher, Government Bilingual  
High School Batouri, Batouri East Region, Cameroon, 2007-  
2011.
- Graduate Teaching Assistant, East Tennessee State University,  
Department of Chemistry, 2012 - 2014.